4-15-2015

Cationic Phenylene Ethynylene Polymers and Oligomers Induce Conformational Changes to Proteins

Gregory Soliz

Gregory A. Soliz
Candidate

Biomedical Engineering Graduate Program
Department

This Thesis is approved, and it is acceptable in quality and form for publication:

Approved by the Thesis Committee:

Dr. Eva Y. Chi, Chairperson

Dr. David G. Whitten

Dr. Andrew P. Shreve

CATIONIC PHENYLENE ETHYNYLENE POLYMERS AND OLIGOMERS INDUCE CONFORMATION CHANGES TO PROTEINS

by

Gregory A. Soliz

Chemical Engineering, Bachelors of Science
2012

THESIS
Submitted in Partial Fullfillment of the
Requirements for Degree of

MASTERS OF SCIENCE
BIOMEDICAL ENGINEERING

The University of New Mexico
Albuquerque, New Mexico

MAY, 2015

CATIONIC PHENYLENE ETHYNYLENE POLYMERS AND OLIGOMERS INDUCE CONFORMATION CHANGES TO PROTEINS

by

Gregory A. Soliz
B.S, Chemical Engineering, University of New Mexico, 2012
M.S., Biomedical Engineering, University of New Mexico, 2015

ABSTRACT

Infectious diseases have been a growing health care concern resulting in added expenses and health care resources to the community. Due to this rising issues research groups have devoted time to resolve this growing issue through the development of various compounds to treat or prevent disease. Research at the University of New Mexico began with trying to kill various strains of bacteria with a novel class of synthetic phenylene ethynylene (PPE)-based conjugated polyelectrolytes (CPEs) has helped in providing a new antimicrobial compound. Results proved successful and lead to experimentation to use the new class of compounds as an antiviral answer as well. The compounds showed high level of inactivation for two model viruses MS2 and T4 bacteriophages. The compound also showed morphological changes to the viral capsids composed of protein assemblies.

Due to the results of previous research the mechanism by which the composed interacted with the protein remained unanswered. Studies were conducted using two model proteins BSA and lysozyme, oppositely charge working in buffers at pH 7.4, to establish a mean by which the compounds affect the proteins. Various spectroscopic techniques were utilized to understand how the proteins are affected on a molecular level. CD was used to examine changes to the secondary

structure of the proteins, fluorescence to examine tertiary structural changes. SDS-PAGE and SEC-HPLC with static light scattering to examine the products of the interaction aggregates or small products then determine the molecular mass of these results.

The CD results showed that BSA was more prone to secondary structural changes. Initial suspected to be caused by the electrostatic interaction between the negative charged BSA and the cationic compounds tested. However, fluorescence results showed similar trends for both BSA and lysozyme leading to more than electrostatics affecting the interaction as the fluorescence results provide information on the tertiary structure for the proteins. Next two separation techniques were utilized to look at how the protein could be chemical altered through cleavage or aggregation. SDS-PAGE provided the first set of results qualitatively showing the compounds cause both aggregation and cleavage in the presence of BSA while lysozyme only showed aggregation. To gather a quantitative result for how this occurred SES-HPLC with static light scattering was used. The results gathered showed that BSA underwent more of an aggregation process with irradiating causing some cleavage of the protein. Lysozyme on the other hand resulted in more cleavage products than aggregates only see effect after irradiation. When gathering all the information it is suspected that the main form for interaction begins with hydrophobic interactions with the compounds trying to keep the backbones away from the solvent environment that would explain why more hydrophobic BSA resulted in more structural change without irradiation.

Table of Contents

List of Figures

1. Background

1.1 Infectious Diseases

Infectious diseases are a growing concern worldwide. Many diseases are caused by bacterial infections. According to the center for disease control in the US, 2 million people become infected with resistant bacterial strains and at least 23,000 die, as a result.[1] Treatment of these infections has been problematic due to the emergence of antibiotic resistant strains. The increased resistance to current antibiotics has also lead to added healthcare cost to the individuals and higher death rates[2]. Due to this expense there is need for a resolution to combat infectious diseases without inducing resistance. Many methods have been developed that range from using silver nanoparticles[3,4,5] to protocells[6,7,8] to overcome the resistance of various strains of bacteria. However, there is still an urgent need for the development of antimicrobial compounds that will not induce resistance.

1.2 CPE/OPEs

The development of a novel class of synthetic phenylene ethynylene (PPE)-based conjugated polyelectrolytes (CPEs) has helped in providing a new antimicrobial compound to combat infectious disease. These compounds have exhibited photo inducible, through UV-visible light exposure, antimicrobial activity. Electron microscopy studies have shown that these CPEs induce morphological changes to *E. coli* cells in **figure 1**[9,10] .Dye leakage assays have shown that the CPEs can selectively permeabilize model bacterial membranes over model mammalian membranes[11]. The CPEs are cationic and amphiphilic, thereby allowing these molecules to interact with and disrupt the structures and functions of biological

macromolecular assemblies such as the lipid membrane, nucleic acids, and proteins. Due to the interactions between CPEs and bacterial membrane[12,13,14,15], it is hypothesized that CPE's ability to disrupt membranes is a major pathway by which these compounds exert toxicity.

Figure 1: SEM images of E. Coli cells incubated for 1 hour with antimicrobial compounds. Yellow arrows showing morphological changes to the cell surface

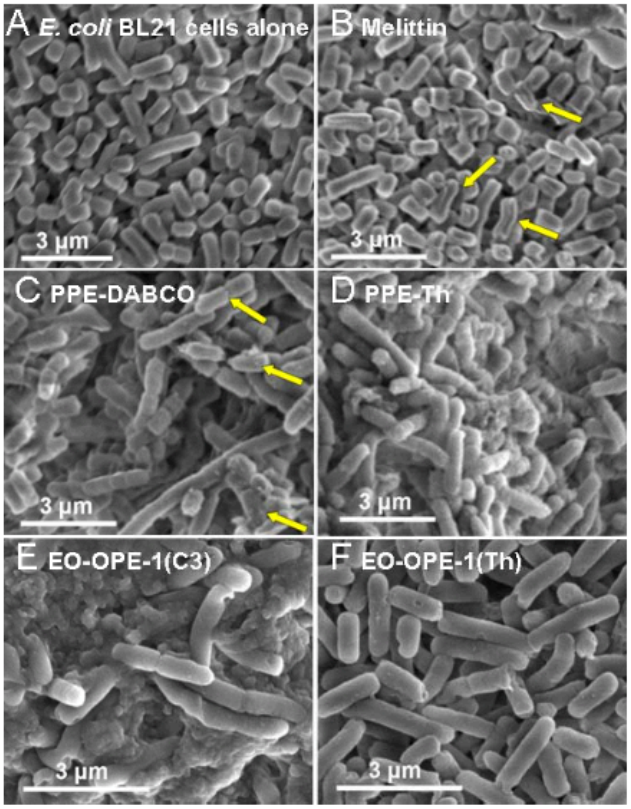

induced by the compounds[9].

Based on the bacterial studies it was believed that the compounds might exhibit similar properties when encountering viruses. Studies were conducted on model viruses to examine if these compounds would provide similar results of inactivation that was seen with the bacterial studies. Two model viruses were tested, MS2 and T4 bacteriophages. Utilizing the photo inducible antimicrobial

activity, the study showed that many of the compounds tested were able to inactivate the bacteriophages with greater levels of inactivation after UV-visible light exposure[16]. SEM images showed that the compound induced morphological changes to the viruses similar to the results seen in bacterial studies. This study established the ability of the compound as an antiviral agent. However, questions were still unanswered as to the mechanism of inactivation.

1.3 Project

Based on the previous studies conducted. There remained an underlining question on how the viruses inactivated. The viruses are composed of a capsid made up of several copies of protein. Research showed that the capsid of the viruses were disrupted. Due to the results of viral capsid studies[16] the compound protein interaction on a molecular level needed to be studied to fully grasp how the compounds work. The studies have been conducted on model proteins Bovine serum albumin (BSA) and lysozyme. Accomplishment of the following three specific aims will aid us in furthering the understanding of the method of disruption for the protein compound interaction.

The compounds chosen shown in **figure 2** were all selected based on results from the antiviral studies conducted on two bacteriophages. The first an end only oligomer (EO-OPE C2) selected for the relation EO-OPE C3 test on the bacteriophages exhibiting higher levels of inactivation than the other oligomers tested. The second and third polymers PPE-Th and PPE-DABCO both were tested against the bacteriophages and displayed high levels of inactivation. The compounds also exhibited the ability to disrupt viral morphology.

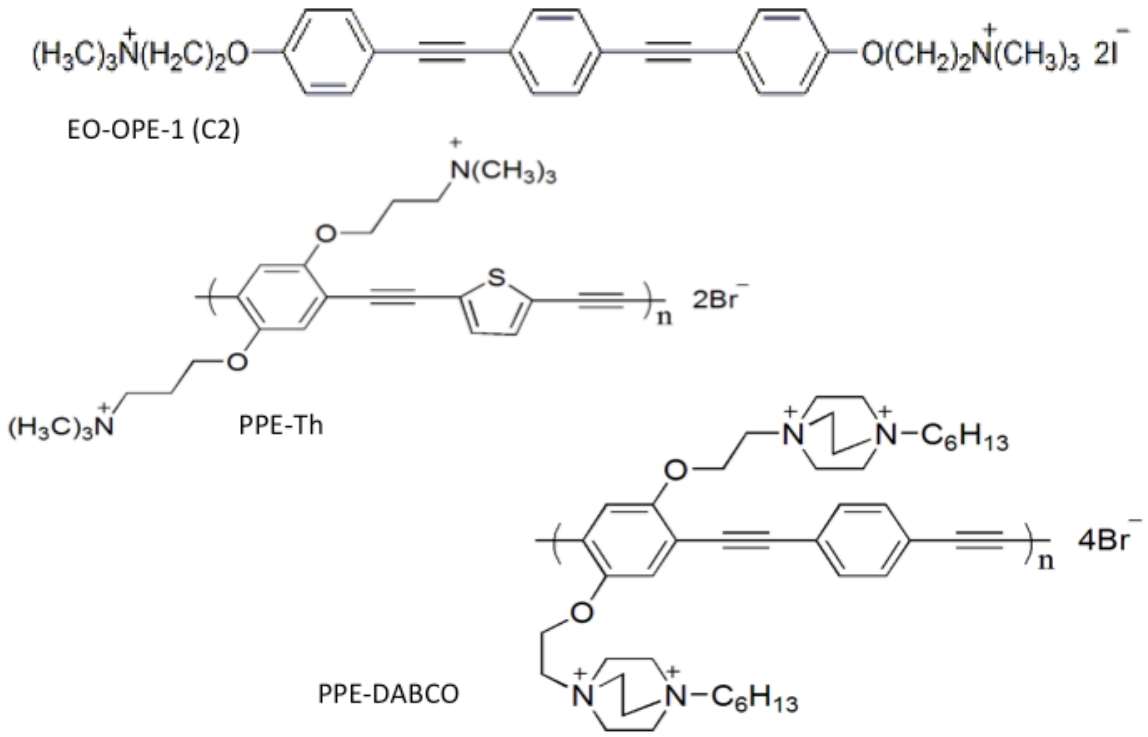

Figure 2: The compounds are all cationic and have been selected based on previous antiviral studies conducted.

Specific Aim 1: Evaluated the structural changes secondary and tertiary on proteins induced by CPE/OPEs

This specific aim focuses spectroscopic techniques to evaluate structural changes to the test proteins and compounds. Far UV circular dichroism has been used to examine the secondary structure of the proteins and how it changes with the compounds tested. The tertiary structure of the protein will be monitored using fluorescence spectroscopy. A change in intrinsic fluorescence of the protein depends on the proteins exposure to the solvent environment caused by structural changes of the protein. Both techniques will be used to analyze how the interaction between the proteins and compound are affecting the structure.

Specific Aim 2: Evaluate the effect of irradiation with protein and CPE/OPEs

All experiments conducted will be done under one of two conditions, dark incubation or irradiation. These treatments will also be conducted on all experiments conducted to monitor any enhanced effects of structural disruption occurs from the irradiation of the compounds. Samples will undergo 1-hour incubation time periods before measurements are taken on CD, fluorescence spectroscopy, SDS-PAGE, and SEC-HPLC with static light scattering.

Specific Aim 3: Evaluate if the proteins undergo chemical alterations in presence of CPE/OPEs

This specific aim will be done in two parts. First SDS-PAGE experiments will be conducted to evaluate how proteins may be aggregated or broken into smaller fragments. The second stage of experiments will be conducted on size exclusion HPLC and will allow the protein that was is in the sample to be fully accounted for using the area under the collected UV chromatograph curve, which is directly proportional to the amount of protein. This technique paired static light scattering will allow us to gather information of what state the protein is in insoluble aggregates, soluble aggregates, small fragments as well as molecular mass of the protein, soluble aggregates, and small fragments. These experiments will also undergo the two incubation treatments.

2. Experimental Theory

When a beam of light strikes a molecule several results may occur, absorbance, transmittance, scattering, reflecting, or fluorescence. This is important because valuable information can be gained about the material being tested from each of these results. Many of these results were measured during experimentation.

Here we will discuss absorption spectroscopy, circular dichroism, fluorescence spectroscopy, SDS-PAGE, SEC-HPLC, and static light scattering.

2.1 Absorption Spectroscopy

Absorption spectroscopy is a process that measures transmittance presents the absorbance of a solution of interest. This technique in the UV spectrum predominantly is for quantitative purposes to determine the amount of compounds present. This is done by gathering absorbance at characteristic wavelength 280 nm, using a molar extinction coefficient, and path length to calculate concentration. Lambert's law illustrates the relationship of incident radiation to transmitted light.

$$I/I_0=T \quad (1)$$

Where:

I= Transmitted light

I_0= Intensity of incident radiation

T= Fraction transmitted

This can be converted to a percent by the following equation

$$I/I_0(100)=\%T \quad (2)$$

Absorbance is then related to transmitted light by the following equation

$$A=\mathrm{Log}_{10}(100/T)=\mathrm{Log}_{10}(I_0/I) \quad (3)$$

Applying the Beer-Lambert law, which states that absorbance is proportional to concentration. It is then possible to collect a reading for the sample and back calculate a corrected concentration for the substance of interest.

$$A=eCl \quad (4)$$

Where the values are given by:

e= extinction coefficient (1/M-cm)

C= concentration (M)

l= path length (cm)

The Beer-Lambert equation was used to calculate the concentrations for all samples run during experimentation. The instrument utilized is a Perkin Elmer Lamda35 UV/vis spectrophotometer in the Chi lab group.

2.2 Far-UV Circular Dichroism

Circular Dichroism (CD) is method that utilizes absorbance in a different manner. CD uses the difference in absorption of the left-handed and right handed polarized light. This difference gives rise to a spectrum that can then be used to determine information about the secondary structure of proteins. CD also follows the Beer-Lambert law as follows[17].

$$\Delta A=A_L-A_R=e_LCl-e_RCl=(e_L-e_R)Cl \quad (5)$$

$$\Theta=2.303(\Delta A)/4l \quad (6)$$

Where:

A= absorbance

L= Left-Hand polarized light

R=Right-Hand polarized light

e= Molar extinction coefficient

l= Path length

Θ= Light that is elliptically polarized.

This can be further manipulated to the final equation:

$[\Theta]= (100\ \Theta M)/(Cln)$

Where:

[Θ]= mean residue molar elipticity

M= molecular mass

C= Concentration

n= number of residues

All experiments conducted were performed on the Aviv 410 circular dichroism spectrophotometer in the Chi lab group.

2.3 Fluorescence spectroscopy

Fluorescence works in conjunction with absorbance. This is because Fluorescence deals with the ability of a molecule to absorb light at certain wavelength then emit light at a different but still specific wavelength. This is all dependent on the molecule and environment the molecule is currently residing. Fluorescence of a molecule can be broken up in a few parts. First excitation of the molecule where absorbed light makes the molecule go into an excited state. Once in the excited state the molecule may undergo conformational or vibrational changes. The part is the release of the collected photon resulting in the fluorescence. This can then be used to look at various molecules, in the case for this project proteins and either oligomers or polymers, to gather structural information.

2.4 Sodium dodecyl sulfate polyacrylamide gel electrophoresis (*SDS-PAGE)*

SDS-PAGE is a widely used separation technique for a variety of molecules such as proteins or nucleic acids. Separation can all be controlled by how the gel is produced. The electric field being applied is what will move proteins in a direction. The direction is dependent on the charge of the protein. SDS is a detergent that will

bind uniformly and unfold proteins giving them a net negative charge proportional to size. This along with the electric field being applied to the gel will move the protein from the negative cathode to the positive cathode separating the proteins based on charge proportional to size and how easily the proteins can move through the gel matrix.

The polyacrylamide gel is constructed to have the resolving portion of the gel where the separation will occur and the loading portion. Generally this loading portion will consist of 4% acrylamide while the bottom-resolving portion is dependent on the samples being run. The percentage of the resolving get is determined by adjusting the concentration of acrylamide and crosslinking agent to control the pore size.

Along with SDS, a second denaturant is added to proteins to reduce disulfide bonds. In these experiments β-mercaptoethanol is the product used to reduce the disulfide bonds of proteins. A final boiling step is usually used to further unfold the proteins.

2.5 Size exclusion HPLC

Size exclusion HPLC is another technique that takes advantage absorbance in the detection process. However, the most important part of the technique is the fact that SEC-HPLCE is a more precise separation method. As in SDS-PAGE, SEC-HPLC relies on the size of the molecule for the separation. Unlike SDS-PAGE no denaturants or reducing agents need to be used in the separation process. The SEC-HPLC is composed of pumps to allow flow of a running buffer and the analyte, an injector, a column, and a detector. The column is the where the separation process

occurs. The column is packed with silica spheres that have pores running through them. In general larger molecules go around the spheres coming out sooner while smaller ones go through the pores and take longer to exit the column. All of this is governed by thermodynamics and kinetics[18].

Beginning with the free energy change described by:

$$\Delta G^0=\Delta H^0-T\Delta S^0=RTlnk \quad (7)$$

Where:

ΔG^0= Free energy

ΔH^0= Enthalpy

ΔS^0= Entropy

T= Absolute temperature

R= Gas constant

k= Partition coefficient

In an ideal situation there would be no adsorption leading $\Delta H^0=0$ resulting in showing that temperature have little affect on retention:

$$lnK_D= -\Delta S^0/R \quad (8)$$

Where:

K_D= Thermodynamic retention factor

The K_D is a fraction of the accessible pore volume for the analyte resulting:

$$K_D=(V_R-V_0)/V_i \quad (9)$$

Where:

V_R= Analytes retention volume

V_0= Interstitial volume

V_i= Intra-particle volume

Solving equation 8 V_R:

$$V_R = K_D V_i + V_0 \quad (10)$$

SEC-HPLC is not only governed by thermodynamic. Kinetics also contributes a big factor on how separation occurs. Starting with the Van Deemter equation:

$$H = ad_p + bD_m/u + cud^2_p/D_m \quad (11)$$

Where:

H= Plate height

a= Particle shape

d_p= Particle diameter

b,c= Constants

D_m= Diffusion coefficient

u= Velocity

Note that generally for proteins b is neglected which leads to the approximation in equation 7.

The diffusion can be calculated as:

$$D_m = 8.34(10^{-10})T/(\eta M^{1/3}) \quad (12)$$

Where

T= Temperature in Kelvin

η= Mobile phase viscosity in Poise

M= Molecular weight of protein

One final note is that resolution of multiple analytes is dependent on the length of the column, linear velocity, and pore volume. The detector will collect UV absorbance of the solution over a given time period. The collected UV chromatograph will be used to determine the amount of protein in various states such as native protein, soluble aggregates, fragments, and insoluble aggregates. The HPLC used is part of the Chi group lab and all experiment and analysis was conducted on the equipment.

2.6 Static Light Scattering

This final experimental technique takes advantage of the light scattered from a molecule of interest. Beginning with basic equation presented by Debye-Zimm[19]

$$K_c/R_\theta=(1+2A_2c)/[MP(\theta)] \quad (13)$$

Where:

K= Experimental constant

R= Rayleigh excess ratio at angle θ

A_2= Thermodynamic non-ideality coefficient

c= Solute concentration

M= Molecular mass

P(θ)= Form factor

An assumption that light is not reflected at the medium particle boundary or attenuated in the particle making equation 13 true only if Rayleigh-Gans-Debye criteria is satisfie

$$|n/n_0-1|<<1 \text{ and } (4\pi n_0/\lambda_0)d|n/n_0-1|<<1 \quad (14)$$

Where:

n= refractive index of solution

n_0= refractive index of solvent

λ_0= Incident wavelength

d= Maximum dimension of the particle

Using the Guinier approximation R_g can be calculated which is the radius of gyration by this relation:

$$\ln P(\theta)=1-(R_g^2/3)q \quad (15)$$

Where:

q= wave vector

A plot of the correct R vs q^2 will result in the slope of $(R_g^2/3)$ allowing for an easy calculation of the radius of gyration. Another important method for determining important parameters such as molecular mass and radius of gyration is a zimm plot.

$$K_c/R_\theta=1/M(1+(R_g^2/3)q^2) \quad (1+2A_2) \quad (16)$$

Where:

M= Molecular mass

This equation can then be plotted against q^2. A linear interpolation can be used to determine the intercept, which will be the inverse of the molecular mass. The slope will be related to the radius of gyration. Equipment now comes standard with software to automatically acquire these terms. The experiments and analysis were performed on equipment from the Chi lab group.

3. Materials and Methods

3.1 Absorption Spectroscopy

To ensure accurate measurements were conducted for the experiments conducted, UV absorption was utilized to first correct protein concentration. The three proteins corrected were lysozyme, BSA, and a recombinant *Bacillus anthracis* spore coat protein (rBclA). A stock solution was made in 10 mM phosphate buffer pH 7.4 for both lysozyme and BSA. The spore coat protein was store at 12 mg/ml in PBS with 20% glycerol. The proteins were diluted with the phosphate buffer to 100 μg/mL and measured absorbance at 280 nm on the UV-vis spectrometer. The absorption values were recorded and applied to Beer-Lambert equation along with the appropriated extinction coefficient for each protein to back calculated the concentration of the stock solutions. After the corrected protein concentrations were calculated the stock was separated into several 500 μl aliquots and stored at -20° C until needed for experimentation.

Absorption spectroscopy was also used to locate the wavelength of highest absorption for the various compounds under two treatments. The first treatment, dark incubation, the compound diluted in 10 mM phosphate buffer (10 μg/mL) and allowed to equilibrate at room temperature in the dark for 1 hr. The second treatment was irradiation of the sample under 420 nm or 350 nm-centered lamps in a Luz chem photochamber for 1 hr. The compounds were then measured on the UV-vis spectrometer using the wavelength program with readings gathered between 200-500 nm. The peak absorption values were then used to select the parameters for the experiments performed following the absorption experiments.

3.2 Fluorescence Spectroscopy

Fluorescence experiments were conducted for various samples to show how the proteins tertiary structure changed in the presence of the various compounds tested, shown in **figure 2,** as well as photo physical changes to the compounds tested. The first sets of experiment conducted on the fluorescence spectrometer were emission spectra gathered between 300-500 nm at an excitation wavelength of 280 nm characteristic of proteins. This was to gather information on the samples that were prepared at a 10:1 mass of protein to compound ratio. Protein or compound controls were also used to monitor changes from baseline. The stock protein solutions were diluted in 10 mM phosphate buffer at pH 7.4 with the compound to be tested. The samples would then undergo one of two treatments dark incubation stored at room temperature for 1 hr or irradiation under the appropriate light source for 1 hr. The sample was then run on the fluorescence spectrometer and the emission spectra collected. The emission spectra of the protein are caused by intrinsic fluorescence of aromatic residues. Changes to the emission spectra may be due to several causes for example FRET, tertiary structural protein changes, or microenvironment changes.

The second set of experiments conducted was to track changes to the proteins tertiary structure as well as any conformational changes to the compounds tested. The samples were prepared the same way at a 10:1 ratio with the emission spectra gathered between 300-500 nm. However, the excitation wavelength values used varied based on the compound used in the samples. The excitation wavelength ranged from 410-326 nm depending on the compound and treatment used. These excitation values correspond to the absorption maxima gathered previously. The

changes to emission spectra for the compounds are indicative of aggregate formation, photo cleavage products, or microenvironment changes.

Molecule of Interest	Dark incubation	Irradiation incubation
Protein	280 nm	280 nm
PPE-DABCO	410 nm	383 nm
PPE-Th	410 nm	378 nm
EO-OPE C2	326 nm	326 nm

Table 1: Shows the excitation parameters used during emission scans of collected data.

3.3 Far-UV Circular Dichroism

The Far-UV circular dichroism was used to determine secondary structural changes to the proteins being tested. Samples were prepared in the same manner as the previous experiment using a 10:1 mass ratio (100 µg/mL protein & 10 µg/mL compound). Protein and compound controls were also used to monitor changes from baseline. 400 µL were loaded into the quartz cuvettes and placed in the instrument. The equipment is cooled via recirculating water cooler to keep the temperature at 25±0.5° C. The data was collected between 200-500 nm with a step size of 0.5 nm. The key peak of interest occurs near 220 nm and is associated with alpha helices. A decrease in this signal is indicative of secondary structural changes. Due to the fact that circular dichroism measures the difference in absorption between left and right polarized light it was important to also monitor the range for the compounds tested to see if any changes occurred.

3.4 SDS-PAGE

SDS-PAGE experiments were conducted as a first pass look at how the tested proteins may be chemically altered. Samples were prepared at a 10:1 mass ratio of protein to compound. Protein and compound controls were also used to monitor changes. A 10% precast gel purchased from Bio-Rad was used in all the experiments. The samples undergo one of two treatments dark incubation or irradiation in the photochamber for 1 hr. The samples are then mixed with the loading dye consisting of 1.2% SDS mixture and heated for 10 min at 90°C. A volume of 50 µL is loaded in the gel wells to have a final protein content of 10 µg. The gel is run at 130 V until completion. Once the run has finished the gel is collected and stained in a coomassie blue solution. A de-staining solution is used to remove excess dye the gel collects to visualize only the protein. The gels are then preserved in a cellophane air-drying kit for imaging.

3.5 Size exclusion HPLC

SEC-HPLC was used in tandem with static light scattering to gain a better understanding of the proteins size distributions and what form the protein is in. Samples were prepared at a 10:1 mass ratio of protein to compound. Protein and compound controls were also used to monitor changes. The two treatments used are dark and irradiation incubation for 1 hour. 100 µL were loaded into the auto sampler vials to inject a total of 100 µg of protein into the column. The running buffer utilized is a phosphate buffer at pH 7.4 with a 137 mM NaCl and 3 mM KCl. The samples were run and data collected over each 60 min run. The data was then analyzed using the Agilent software to properly integrate the area under the curves

to determine the percentage of protein in native form, insoluble aggregates, soluble aggregates, and fragments.

3.6 Static Light Scattering

Static light scattering was done in tandem with SEC-HPLC to determine the molecular mass of the larger aggregates that may have formed during the incubation period or smaller products. The sample is run through the SEC-HPLC first and then flows through the Dawn Heleos-II and the Optilab rex from Wyatt technology hooked up in tandem. The data is collected and analyzed using the Astra6 software.

4. Results

4.1 Circular dichroism

Circular Dichroism experiments were conducted on all proteins of interest (BSA, lysozyme, rBclA) to examine the effect on secondary structure. Following the protocol-listed in section 3.3 the samples were prepared accordingly. To account for variability between cuvettes the samples were loaded into the cuvette allowed to incubate for the current treatment either dark or irradiation. Once the incubation period ended the sample was run on the Aviv 410 and data collected following this run the sample would then undergo the remaining treatment in the same cuvette. This allowed the variations between cuvettes as well as sample preparation used to be minimized. All sample data was collected between 200 and 600 nm to determine the effect on protein structure as well as monitor any possible induced chirality for the compounds.

Figure 3 shows CD spectra undergoing the various treatments with PPE-Th. This was conducted at a 10:1 mass ratio with a total volume of 400 µl. The inset

graph shows induce chirality for the polymer when in the presence of BSA. The polymer is responsible for this signal because the protein does not absorb within 400-500 nm. The results for this set show that BSA has strong α-helical signal given by the bands at 222 nm and 208 nm. The BSA that has undergone irradiation follows the control BSA spectrum. The compound alone does not produce any signal within this region as shown in green. The samples resulted in interesting outcome with the dark incubation reducing the signal intensity. Radiation further enhanced the polymers ability to destabilize the secondary structures of BSA. The results for PPE-DABCO were similar to that of PPE-Th with the exception that the PPE-DABCO had no effect on the protein in the dark alone. Only with irradiation was PP-DABCO able to destabilize the secondary structure of BSA as shown in **figure 4**. **Figure 5** shows how the oligomer destabilized BSA. Of the compounds test only PPE-Th had induced chirality with BSA.

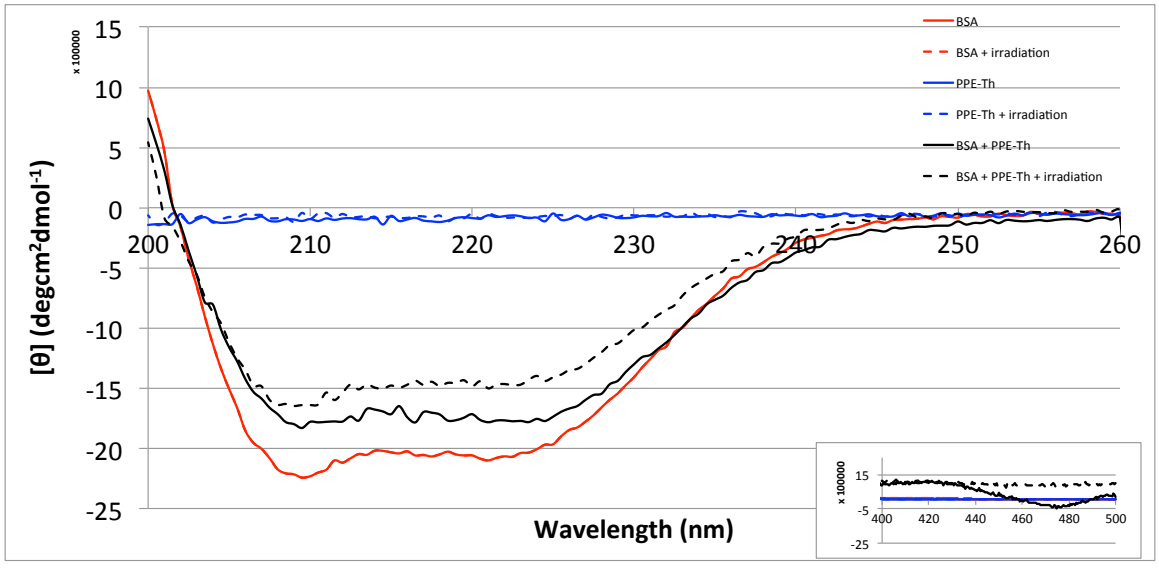

Figure 3: The CD spectrum of BSA controls, PPE-Th controls, and Samples at 10:1 mass protein to compound ratio. Irradiation shows no effect on BSA alone. The

compound PPE-Th in dark is able to reduce the signal intensity with the addition of irradiation an enhancing the effect occurs. The inset graph shows the induced chirality from PPE-Th when in the presence of BSA.

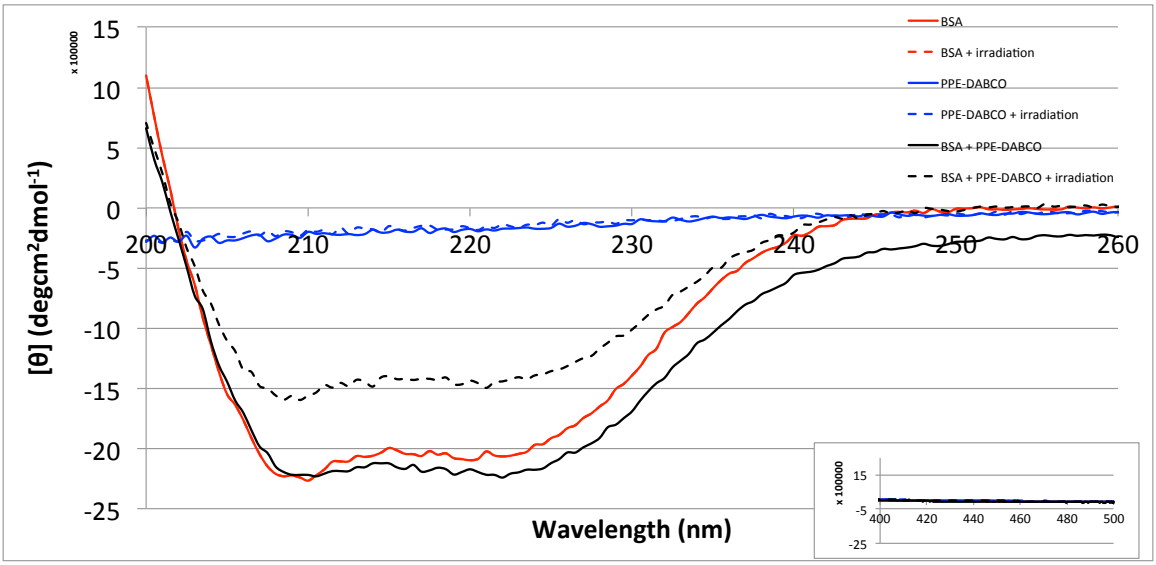

Figure 4: The CD spectrum of BSA controls, PPE-DABCO controls, and Samples at 10:1 mass protein to compound ratio. Irradiation shows no effect on BSA alone. PPE-DABCO in dark is unable to reduce the signal intensity for BSA. Irradiation will allow PPE-DABCO to destabilize the secondary structure resulting in a reduced signal. The inset graph shows no induced chirality

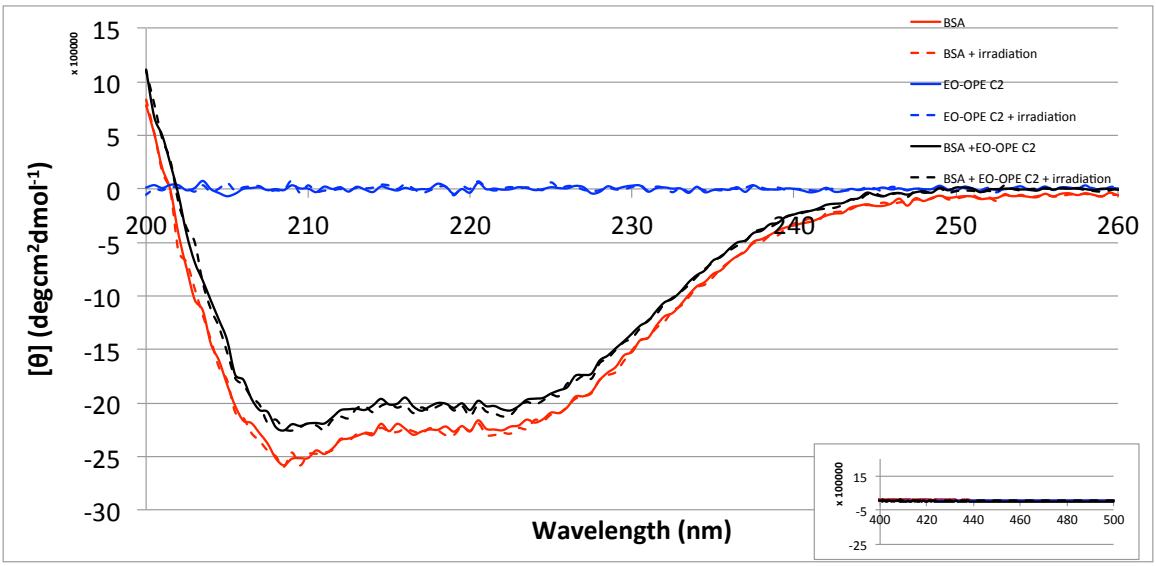

Figure 5: The affect of EO-OPE C2 to destabilize the structure of BSA is small compared to that of the polymers. The addition of irradiation has no effect of enhancement as seen in the polymers.

Figure 6,7,8 show the spectra of lysozyme experiments. Lysozyme experiments were conducted showing results different from those of BSA runs. PPE-DABCO had the opposite effect on lysozyme with dark incubation resulting in an enhancement to the structure of lysozyme. After irradiation of the sample the signal intensity was reduce destabilizing the secondary enhancement that occurred in the dark. PPE-Th had no real effect on the structure of lysozyme in the dark or after irradiation. EO-OPE C2 showed a change similar to that of PPE-DABCO. Irradiation enhances the oligomers ability to disrupt the secondary while in the dark the structure is unaffected.

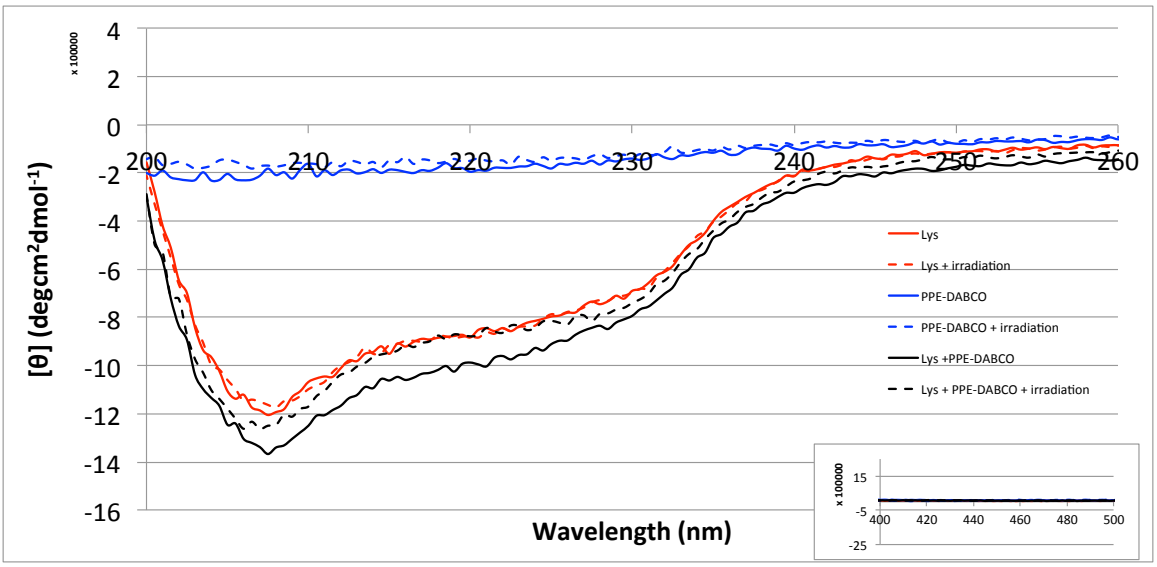

Figure 6: The Cd spectrum of Lysozyme samples with PPE-DABCO being tested. All spectra overlap excluding the dark incubation with PPE-DABCO there seems to be an enhancement of the secondary structure this could be accounted for by variability. The inset graph shows no induce chirality for the polymer.

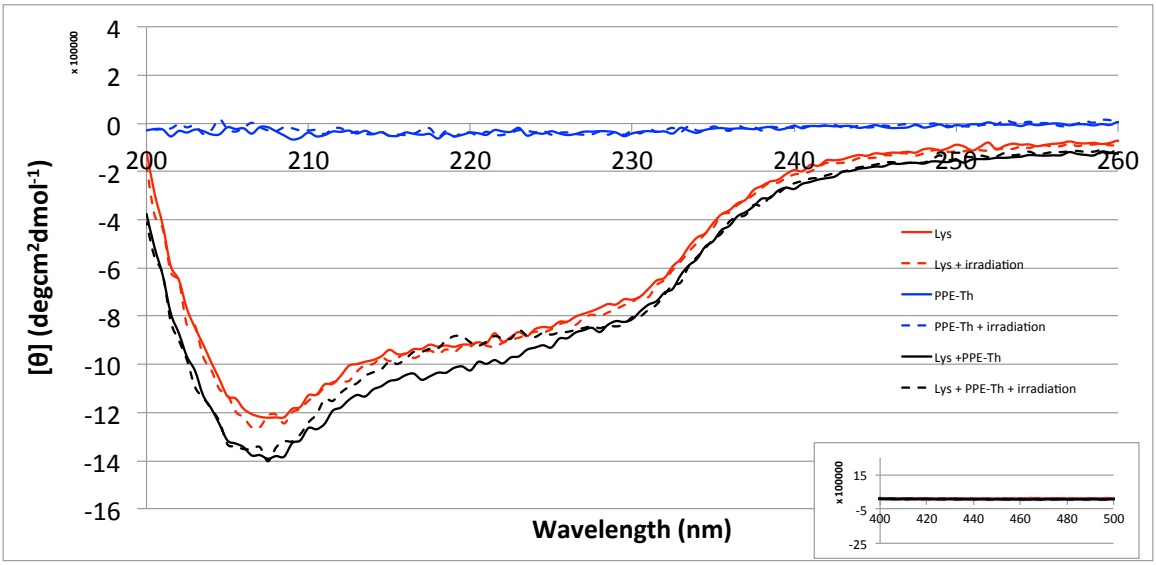

Figure 7: The CD spectrum of Lysozyme samples with PPE-Th being tested. All spectra overlap excluding the dark incubation with PPE-Th there seems to be an enhancement of the secondary structure. The inset graph shows no induce chirality for the polymer.

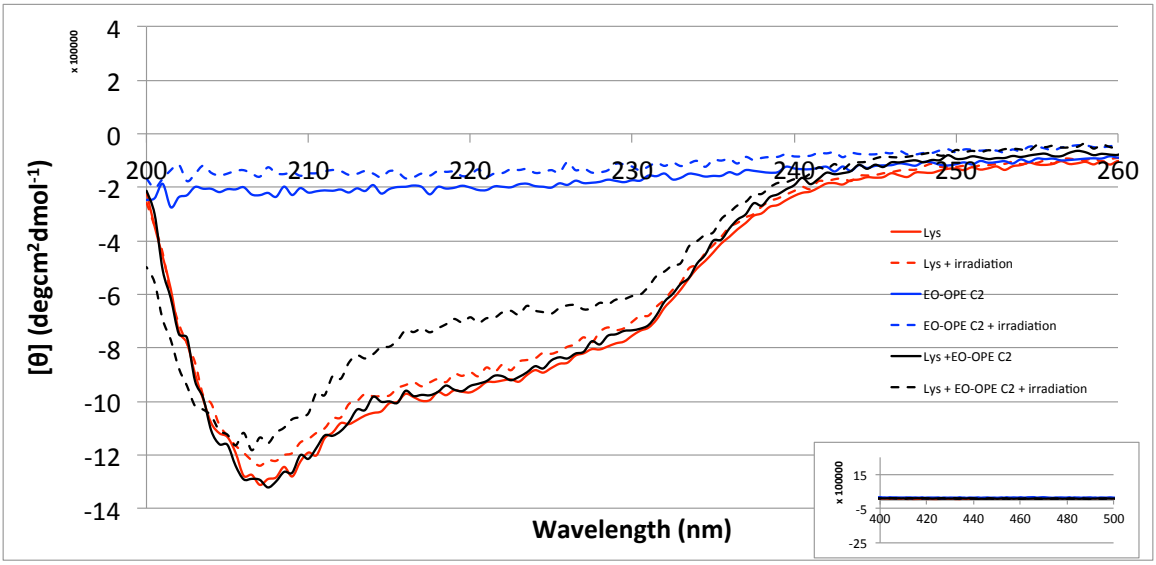

Figure 8: The CD spectrum Lysozyme samples with EO-OPE C2 being tested. All spectra overlap excluding the irradiation incubation resulting in structure destabilization. The inset graph shows no induce chirality for the oligomer.

The experiments conducted on the rBclA spore coat protein were inconclusive due to the issue that there was no signal from the protein to allow for analysis of the potential structure destabilization.

4.2 Fluorescence Spectroscopy

Fluorescence spectroscopy was ran all both BSA and lysozyme with the resulting **figures 9, 10, 11,12, 13, 14** shown below. The experiments were performed following the protocol presented in 3.2 of methods. The samples were loaded at the same concentration and mass ratio used for the CD experiment the volume was 100 µl with the emission scan collected at an excitation of 280 nm.

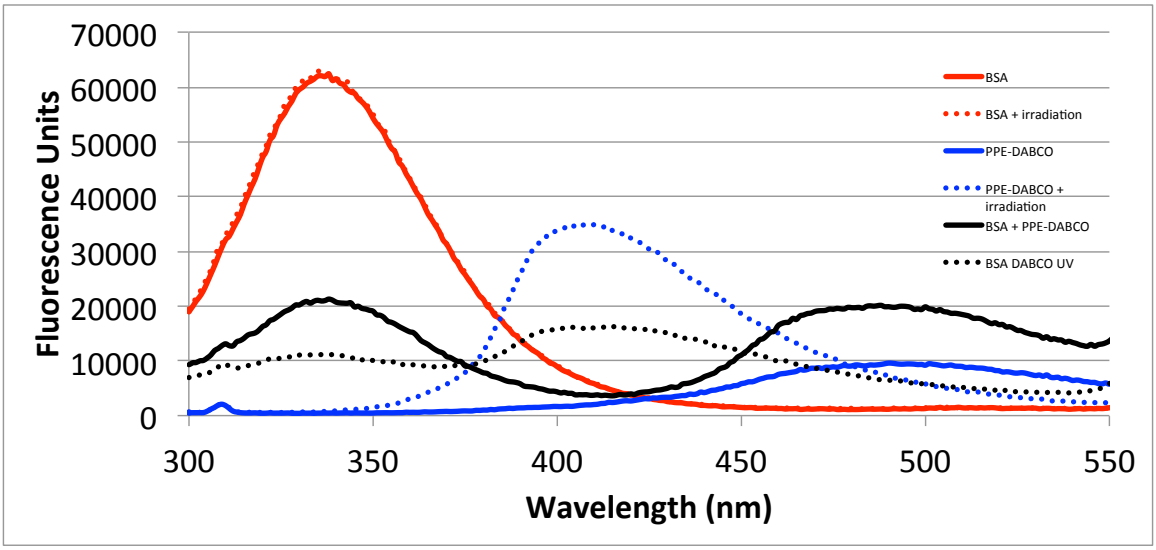

Figure 9: Fluorescence spectra of BSA at excitation 280 nm under various conditions. The intrinsic peak for proteins appears at 340 nm with PPE-DABCO peaks appearing further into the red spectra. The protein alone exhibits a high fluorescence that is then reduced in the presence of the compound shown in red. After irradiation there is blue spectral shift for the compounds and increased intensity.

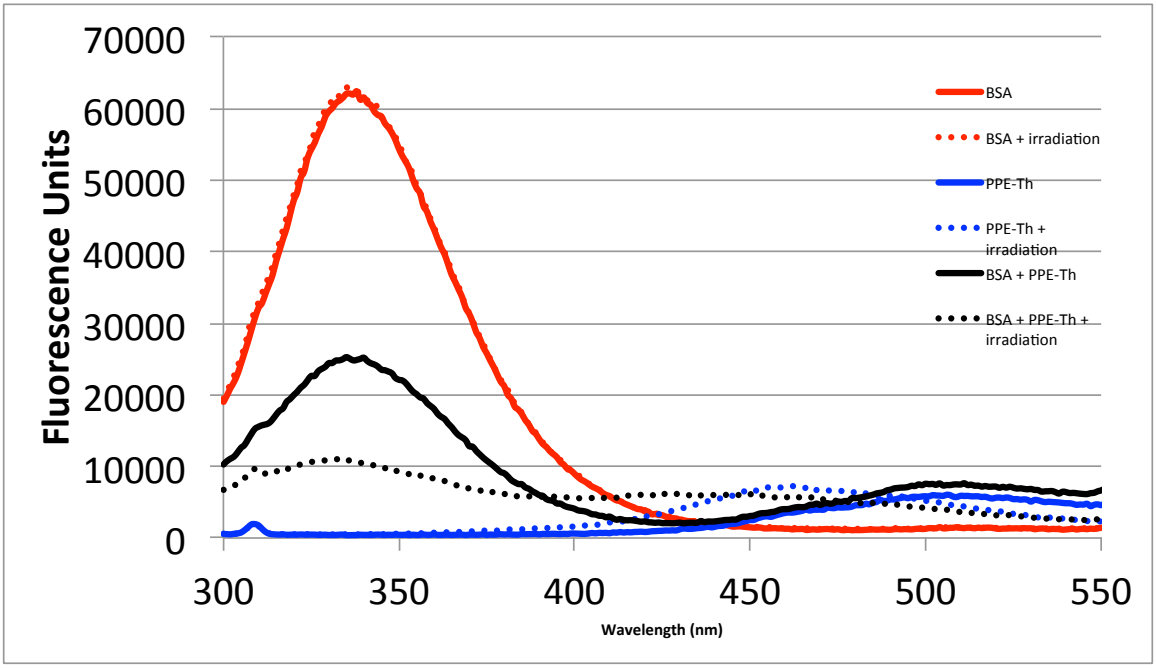

Figure 10: Fluorescence spectra of BSA at excitation 280 nm under various conditions. The intrinsic peak for proteins appears at 340 nm with PPE-Th peaks appearing further into the red spectra. The protein alone exhibits a high fluorescence that is then reduced in the presence of the compound shown in red. After irradiation there is blue spectral shift for the compounds and increased intensity.

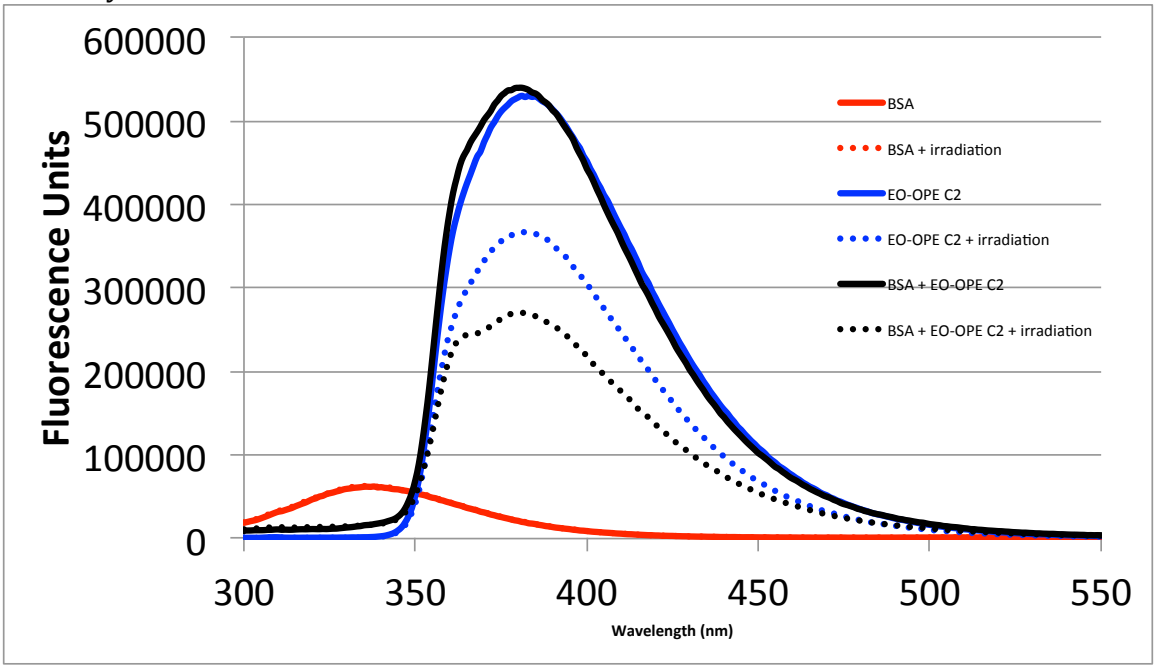

Figure 11: Fluorescence spectra of BSA at excitation 280 nm under various conditions. The intrinsic peak for proteins appears at 340 nm with EO-OPE C2 peaks appearing further into the red spectra. The protein alone exhibits a high fluorescence that is then reduced in the presence of the compound shown in red.

After irradiation there is slight blue spectral shift for the compounds and decreased intensity.

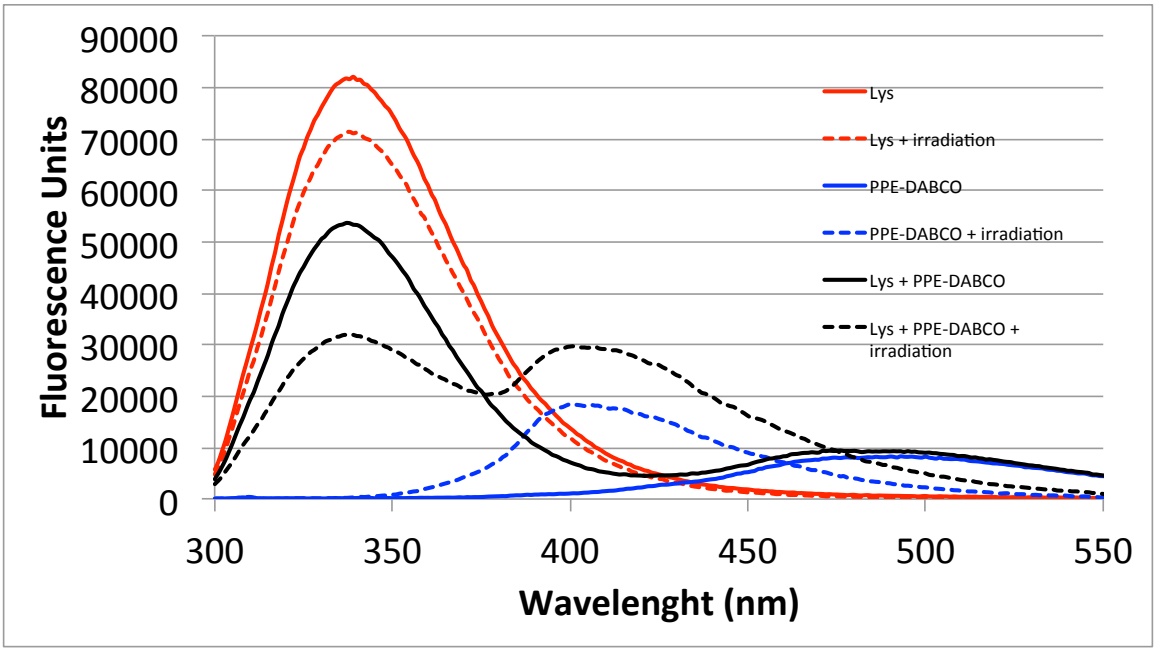

Figure 12: Fluorescence spectra of Lys at excitation 280 nm under various conditions. The intrinsic peak for proteins appears at 340 nm with PPE-DABCO peaks appearing further into the red spectra. The protein alone exhibits a high fluorescence that is then reduced in the presence of the compound shown in red. After irradiation there is blue spectral shift for the compounds and increased intensity. Irradiation also has an effect on lysozyme alone.

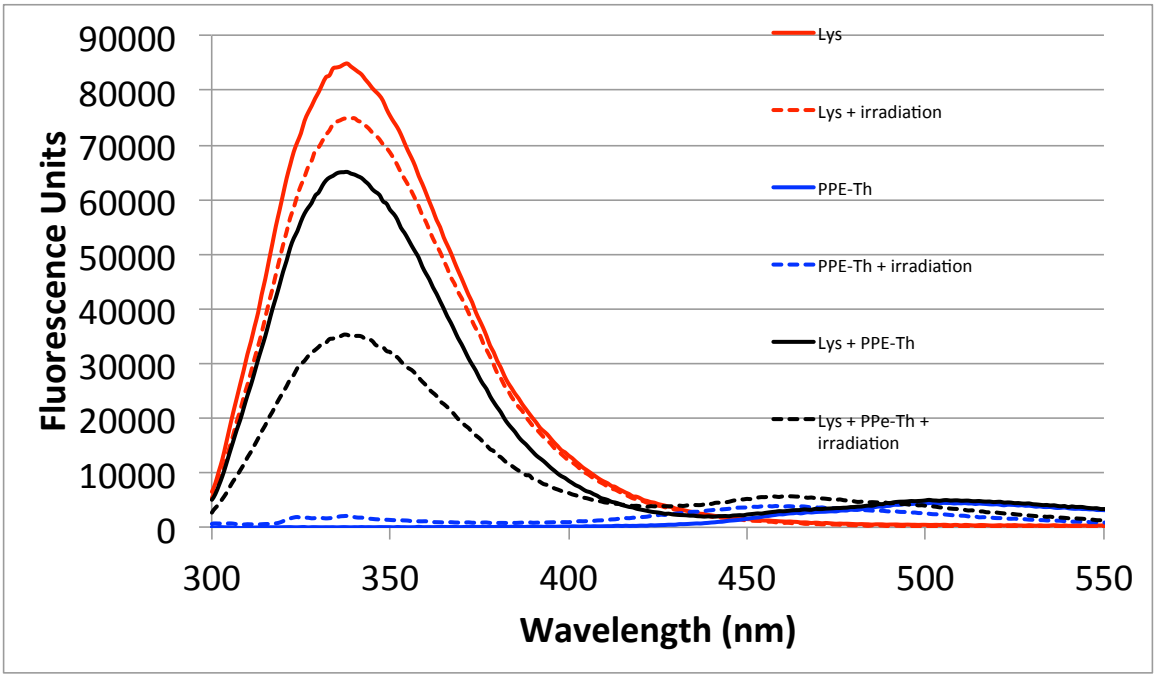

Figure 13: Fluorescence spectra of Lysozyme at excitation 280 nm under various conditions. The intrinsic peak for proteins appears at 340 nm with PPE-Th peaks appearing further into the red spectra. The protein alone exhibits a high fluorescence that is then reduced in the presence of the compound shown in red. After irradiation there is blue spectral shift for the compounds and increased intensity.

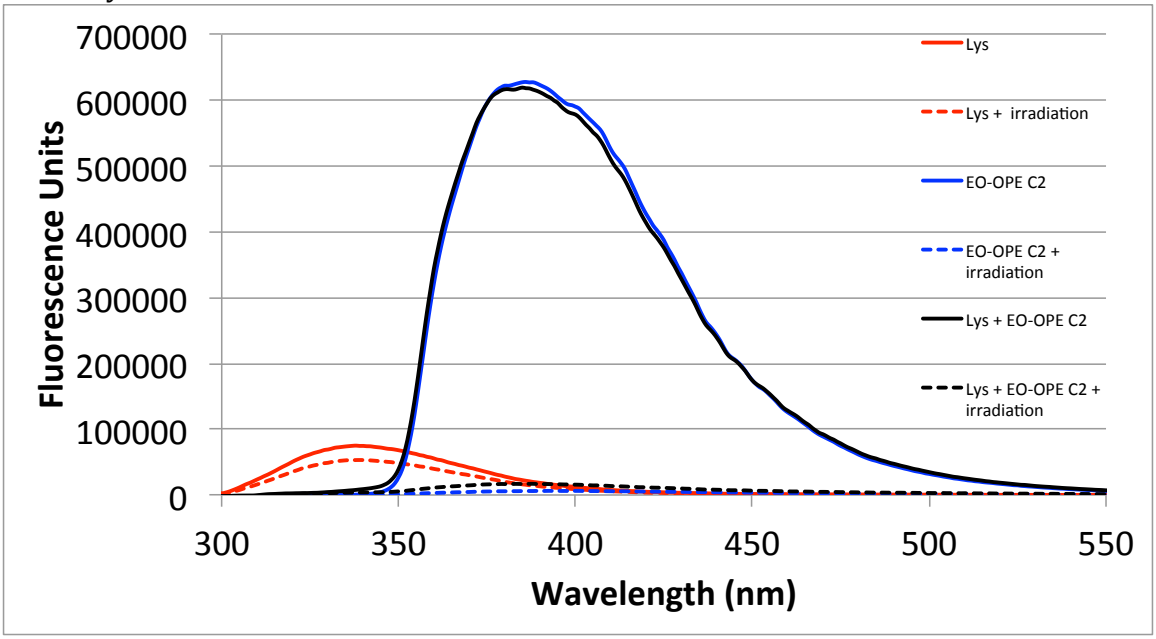

Figure 14: Fluorescence spectra of Lys at excitation 280 nm under various conditions. The intrinsic peak for proteins appears at 340 nm with EO-OPE c2 peaks appearing further into the red spectra. The protein alone exhibits a high fluorescence that is then reduced in the presence of the compound shown in red. The intensity of the compound over shadows that of the protein. However, similar results as with BSA occur for lysozyme.

The Fluorescence data provide proof that the tertiary structure of the proteins is being altered because of intensity reduction from the protein signal at 340 nm. This is show in all the experiment done for fluorescence as the compound is add there is a reduction in the protein amplitude indicative of hydrophobic residues being exposed to the solvent environment.

4.3 SDS-PAGE

SDS-PAGE experiments were conducted on both BSA and lysozyme as a first pass look to see how the tested compounds alter the protein whether by

aggregation or cleavage. A 10% gel was used for BSA for lysozyme a 15% gel was used this is to allow for a better quality gel from each due to the size discrepancy between the two proteins. **Figure 15** shows the results for BSA samples.

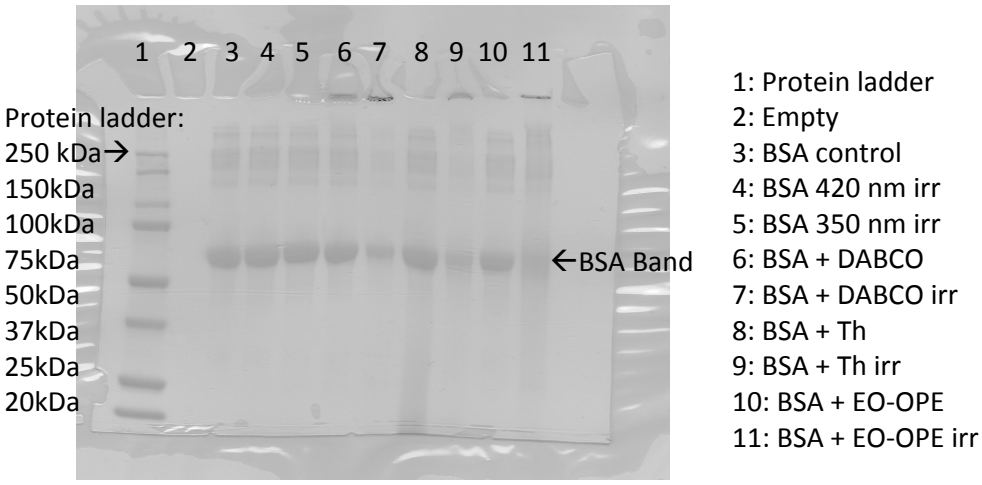

Figure 15: The SDS-PAGE experiment with BSA and all the compounds tested. The BSA band appears where it should near 65 KDa as well as some bands from the purification process resulting in dimers and trimers of BSA. Lanes 6, 7, 9, and 11 have shown aggregation of BSA too larger to enter the gel. Lanes 8 and 11 show cleavage product shown by the smear after the BSA band.

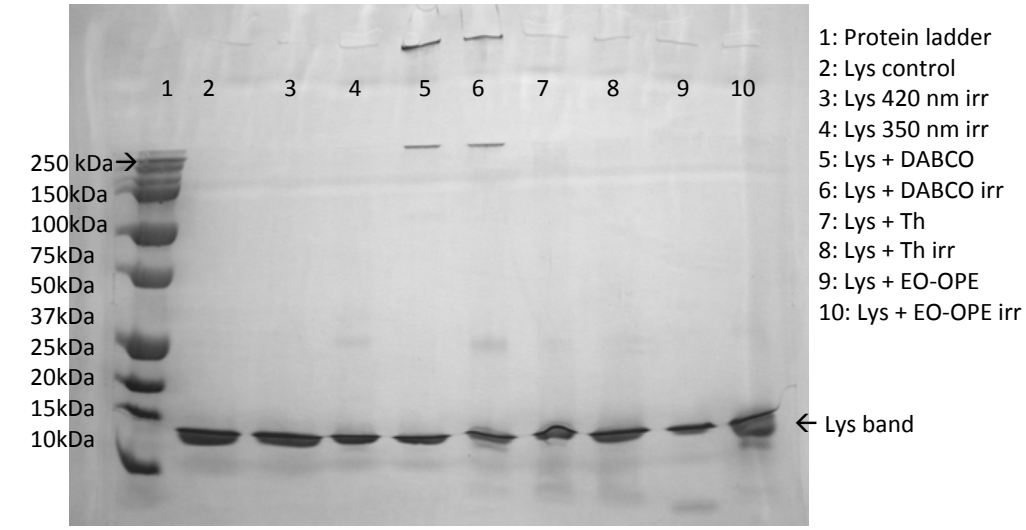

Figure 16: The SDS-PAGE experiment with lys and all the compounds tested. The lys band appears where it should. Lane 5 and 6 have shown aggregation of lys too larger to enter the gel.

Both gel showed results that were not expected. Lysozyme did not have very many changes except in the presence of PPE-DABCO were any changes seen. BSA had both aggregation and cleavage products for the protein as seen in **figure 15.**

4.4 SEC-HPLC and Static light scattering

The system was setup so that the solution would travel through the HPLC and into the Dawn Heleos-II for static light scattering measurement. The samples were prepared to maintain a 10:1 mass protein to compound ratio and allow for 100 µg of protein was loaded onto a BioSep-SEC-s3000 column. **Figures 17-23** are the UV chromatographs from the HPLC for each of the sample sets. **Figure 27 and 28** summarize the results from the HPLC data collected. The data was collected at 280 nm wavelength.

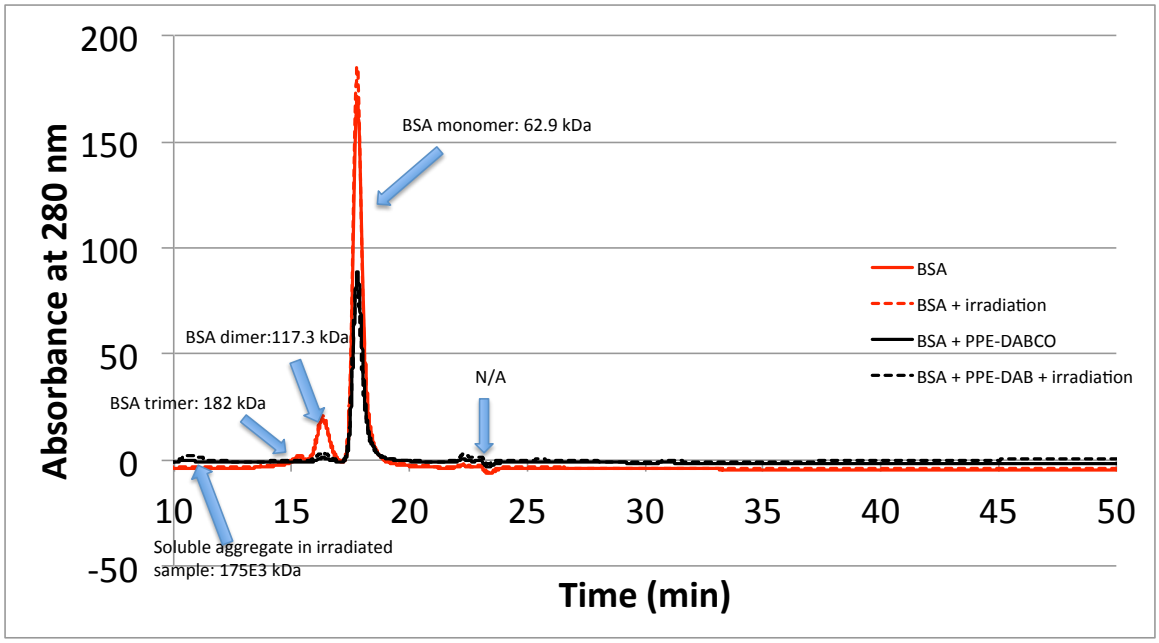

Figure 17: The UV chromatograph comparing the results at 280 nm for BSA controls and samples with PPE-DABCO. The first thing to notice is that the trimer,

dimer, and monomer peak for BSA has been reduced in intensity as well as a peak occurring earlier in the collection process from a soluble aggregate.

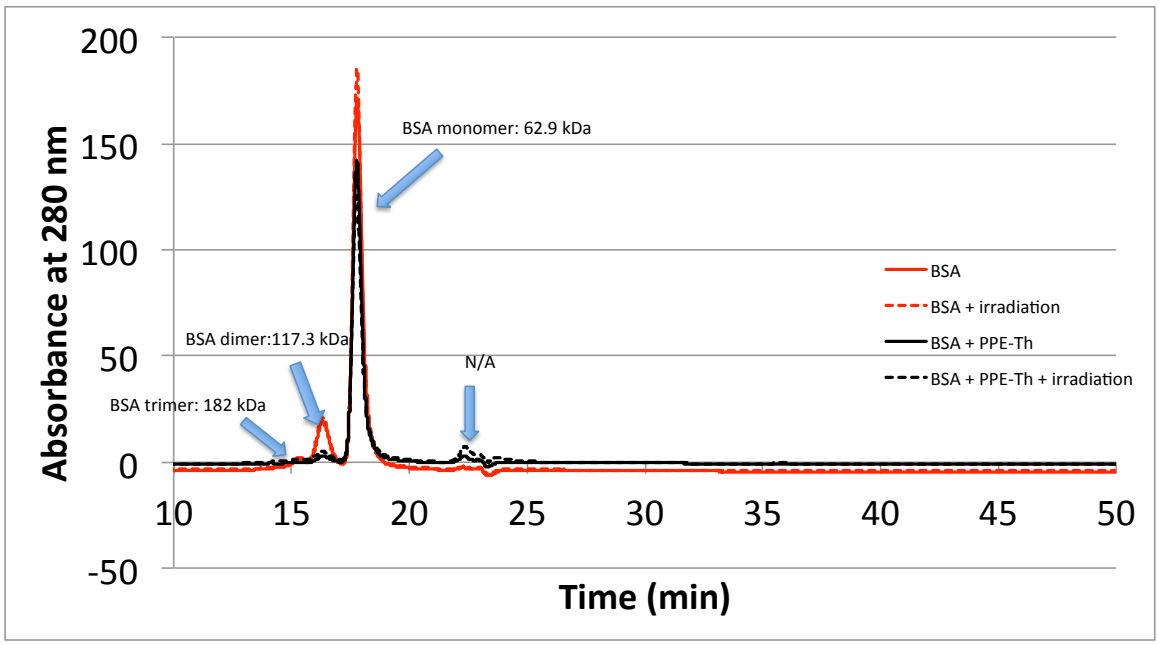

Figure 18: The UV chromatograph comparing the results at 280 nm for BSA controls and samples with PPE-Th. The first thing to notice is that the trimer, dimer, and monomer peak for BSA has been reduced in intensity as well as a peak occurring earlier in the collection process from a soluble aggregate. In both the dark incubation and irradiation samples there are peaks appearing after the monomer peak showing small products.

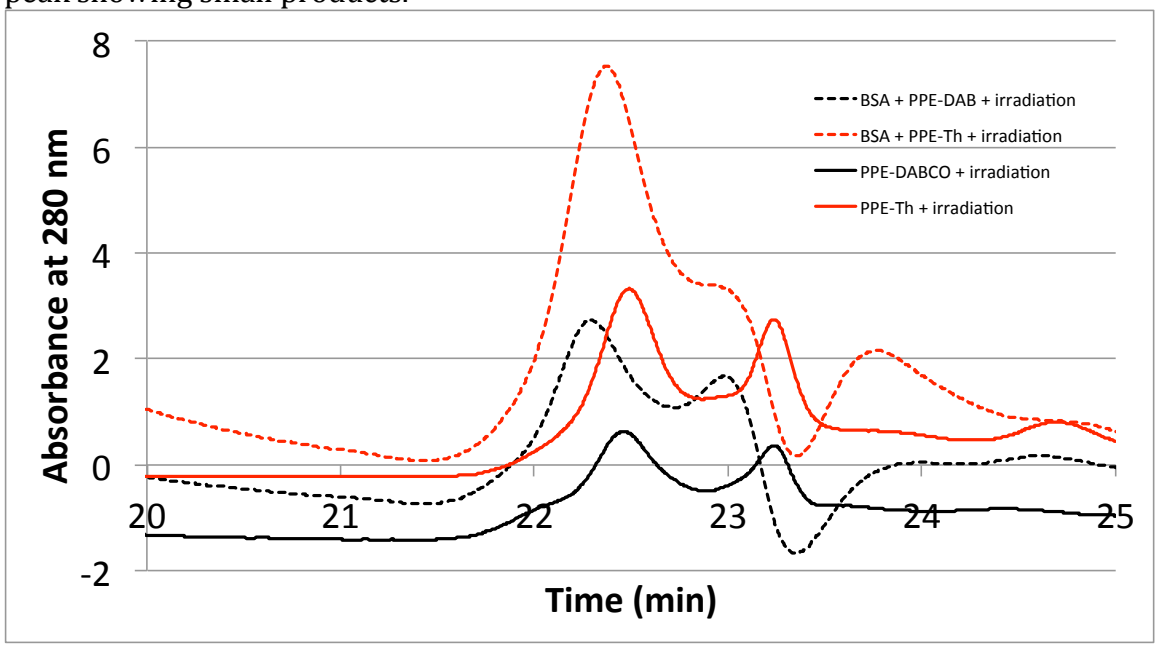

Figure 19: The UV chromatograph comparing the results at 280 nm for BSA samples with PPE-Th and PPE-DABCO after irradiation. The loaded protein is 100 μg

with 10 μg of compound. The compounds show absorbance at 280 nm as seen by the peaks between 22 min and 24 min in solid black for PPE-DABCO and red for PPE-Th. There is a signal enhancement when in the presence of the protein.

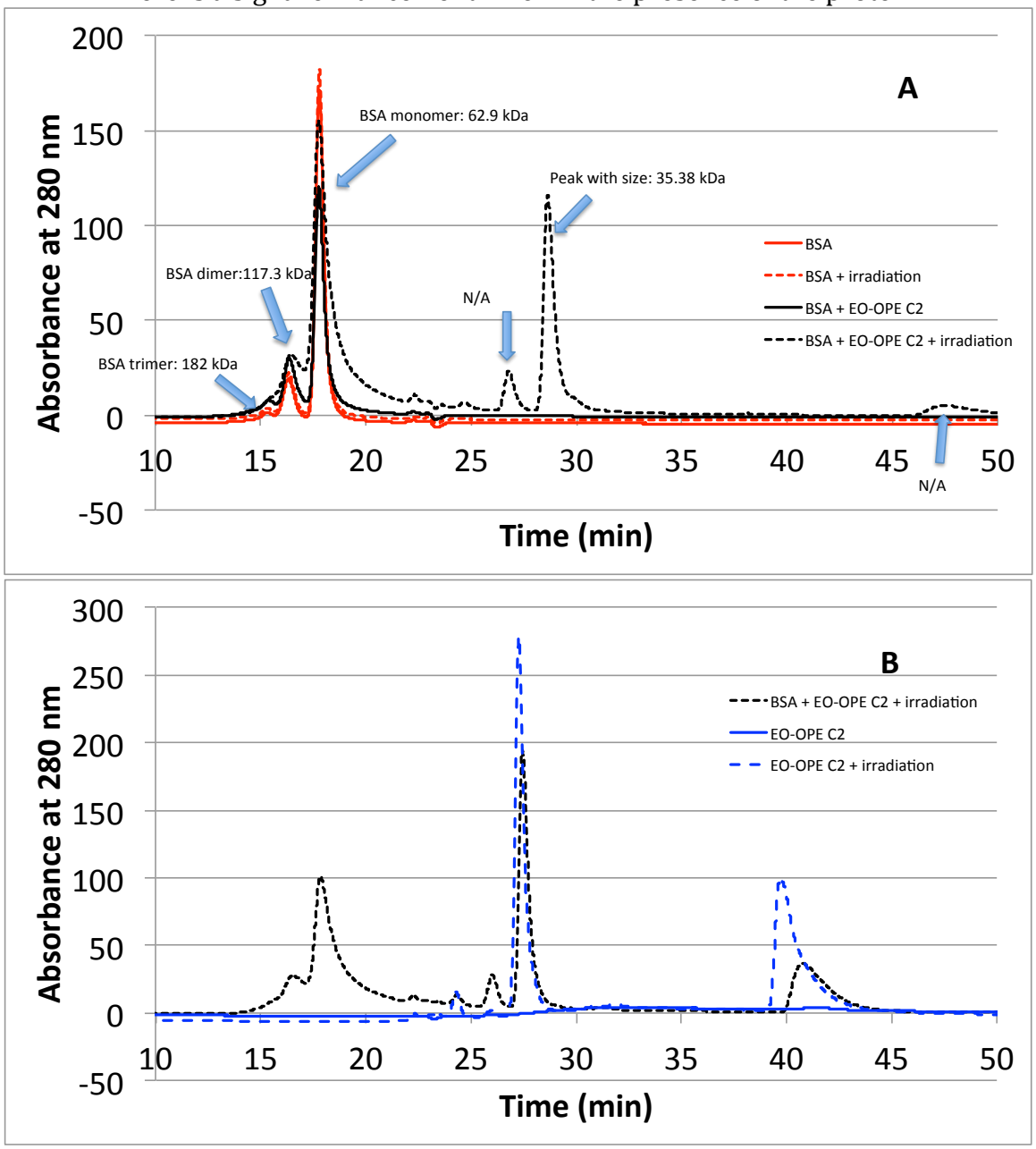

Figure 20: (A) The UV chromatograph comparing the results at 280 nm for BSA controls and samples with EO-OPE C2. The first thing to notice is that the trimer, dimer, and monomer peak for BSA has been combined into a single peak with a shoulder and increased in intensity. In the irradiation samples there are peaks appearing after the monomer peak showing small products. This has been attributed to the EO-OPE C2 those peaks. **(B)** The UV chromatograph comparing the results at 280 nm for BSA with EO-OPE C2 and irradiation to the controls for EO-OPE C2 both in a dark incubation and irradiated sample. From this we see that the compound produces spectra at 280.

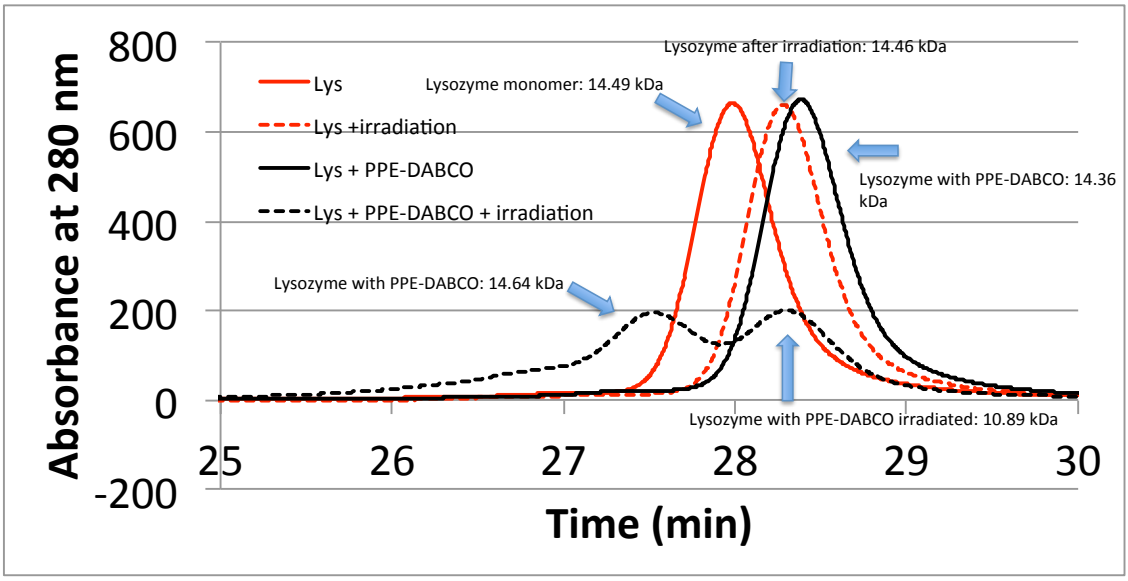

Figure 21: The UV chromatograph comparing the results at 280 nm for lys controls and samples with PPE-DABCO. The irradiated sample with PPE-DABCO begins to form a larger shoulder cause by some soluble aggregates.

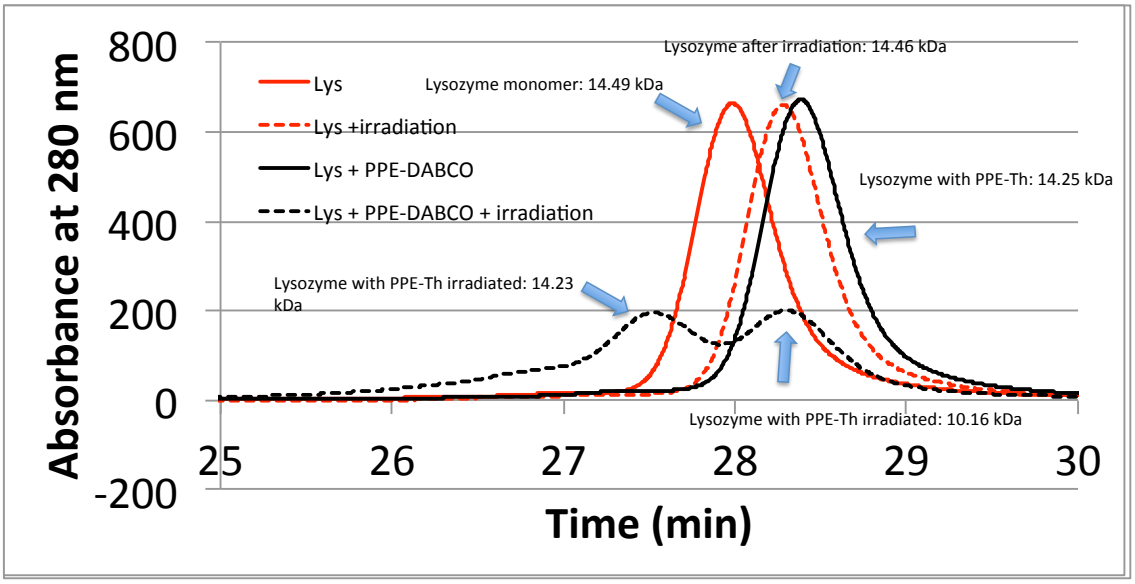

Figure 22: The UV chromatograph comparing the results at 280 nm for lys controls and samples with PPE-Th. The irradiated sample with PPE-Th begins to form a larger shoulder cause by some soluble aggregates.

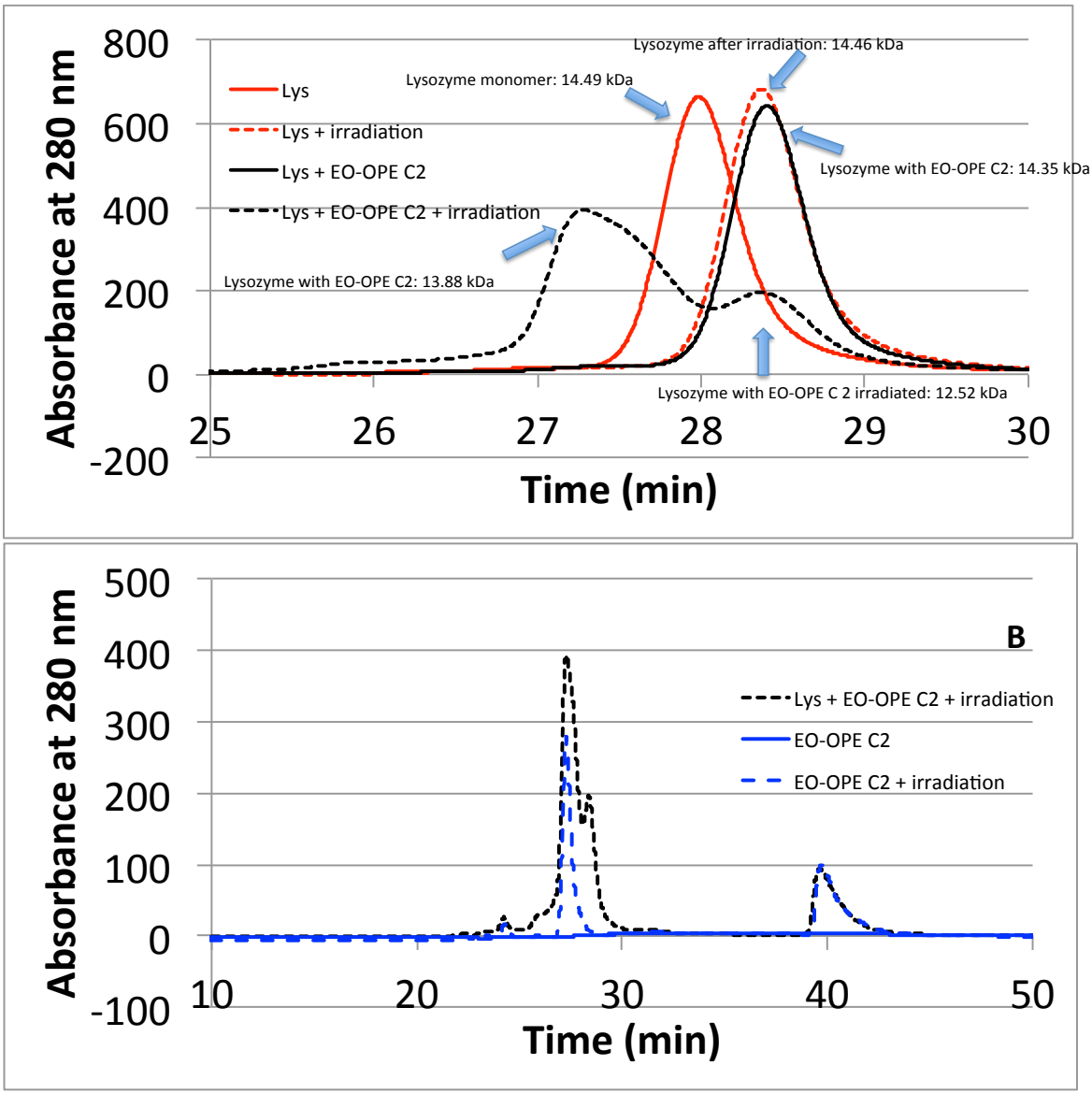

Figure 23: (A) The UV chromatograph comparing the results at 280 nm for lys controls and samples with EO-OPE C2. The irradiated sample with EO-OPE C2 begins to form peaks as seen in the BSA samples caused by the EO-OPE C2. **(B)** The UV chromatograph comparing the results at 280 nm for lys with EO-OPE C2 and irradiation to the controls for EO-OPE C2 both in a dark incubation and irradiated sample. From this we see that the compound produces spectra at 280.

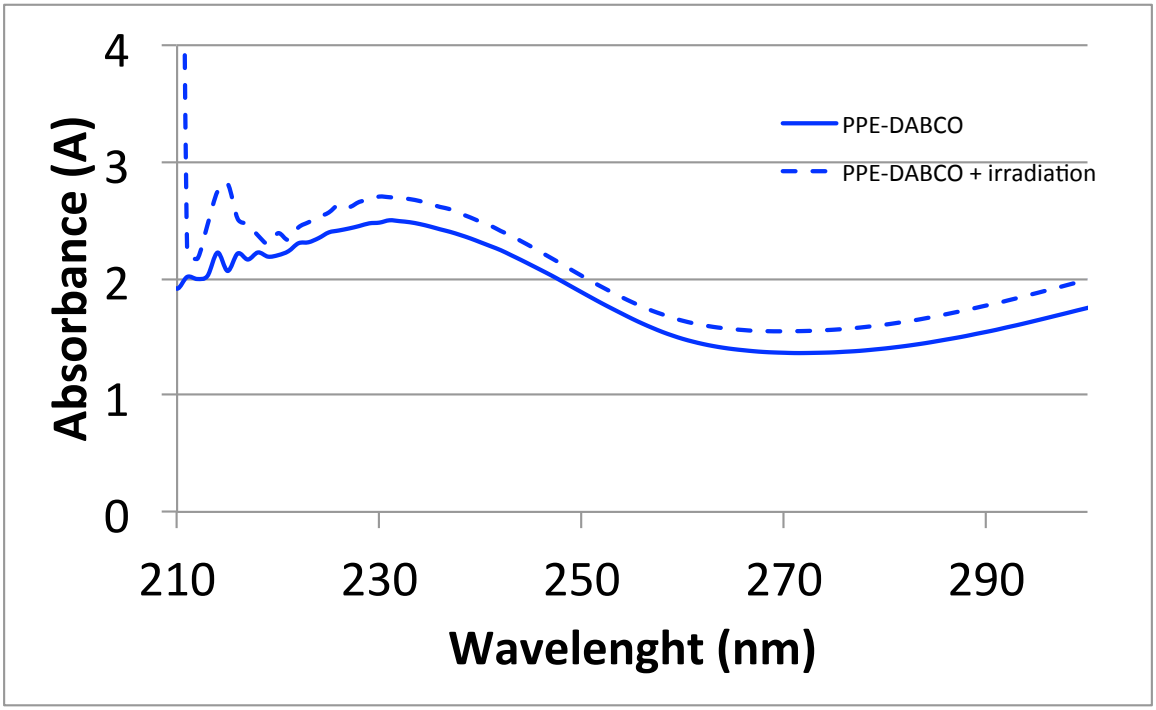

Figure 24: UV spectra of PPE-DABCO controls between 210 and 300 nm to see if the compounds absorb in that region. Near 280 nm PPE-DABCO has the lowest absorbance in the spectra collected. Near 215 nm there is the appearance of a peak and increase of absorbance. There is also increased absorbance after irradiation.

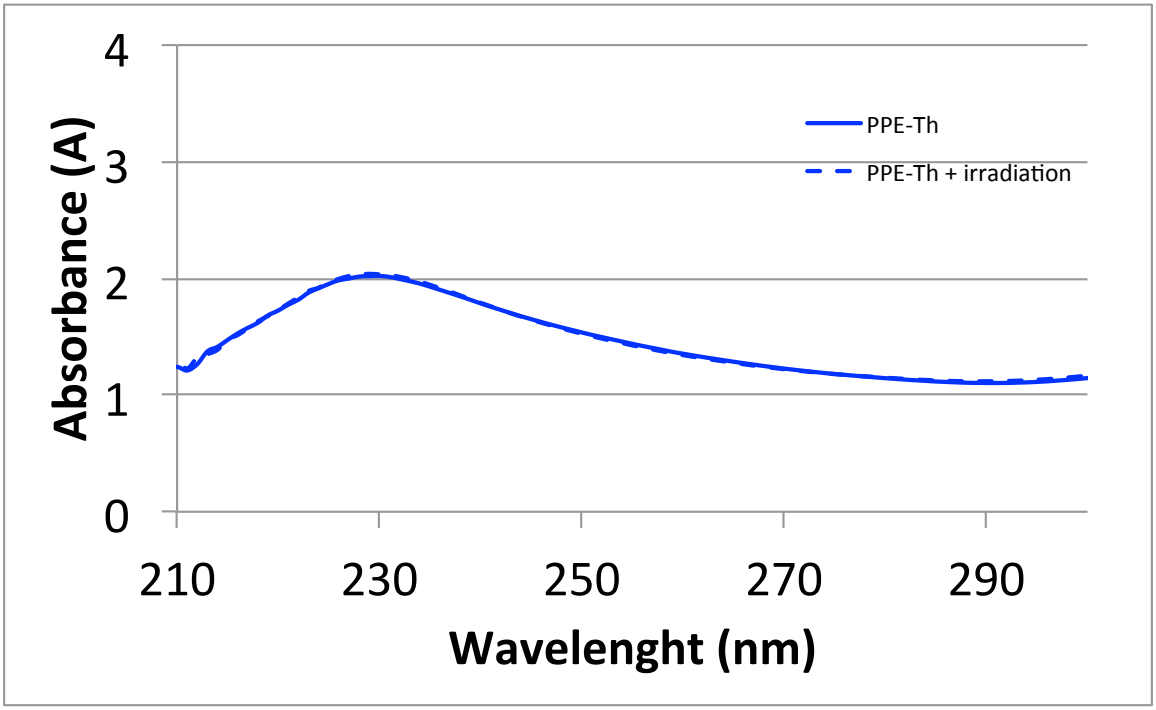

Figure 25: UV spectra of PPE-Th controls between 210 and 300 nm to see if the compounds absorb in that region. Near 280 nm PPE-Th has the lowest absorbance in the spectra collected. Near 215 nm there is the appearance of a peak and increase of absorbance.

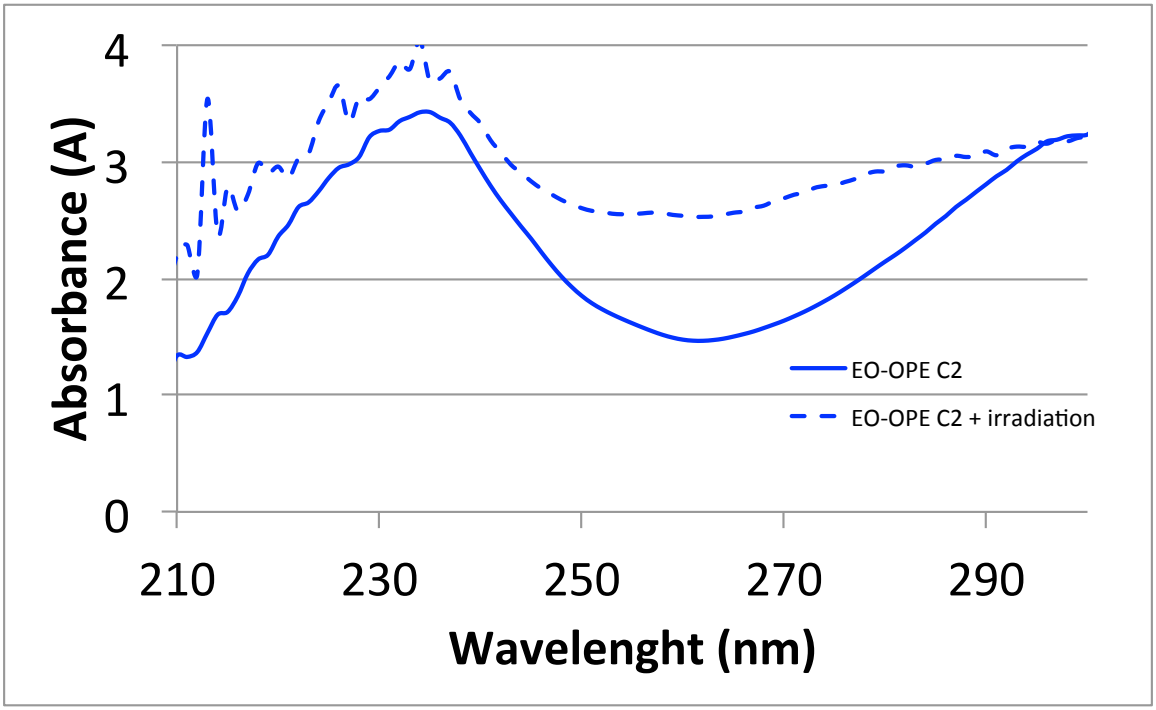

Figure 26: UV spectra of EO-OPE C2 controls between 210 and 300 nm to see if the compounds absorb in that region. Near 280 nm EO-OPE C2 has the lowest absorbance in the spectra collected. Near 215 nm there is the appearance of a peak and increase of absorbance. After irradiation of the compound there is an increase of absorbance near 280 and 215 nm.

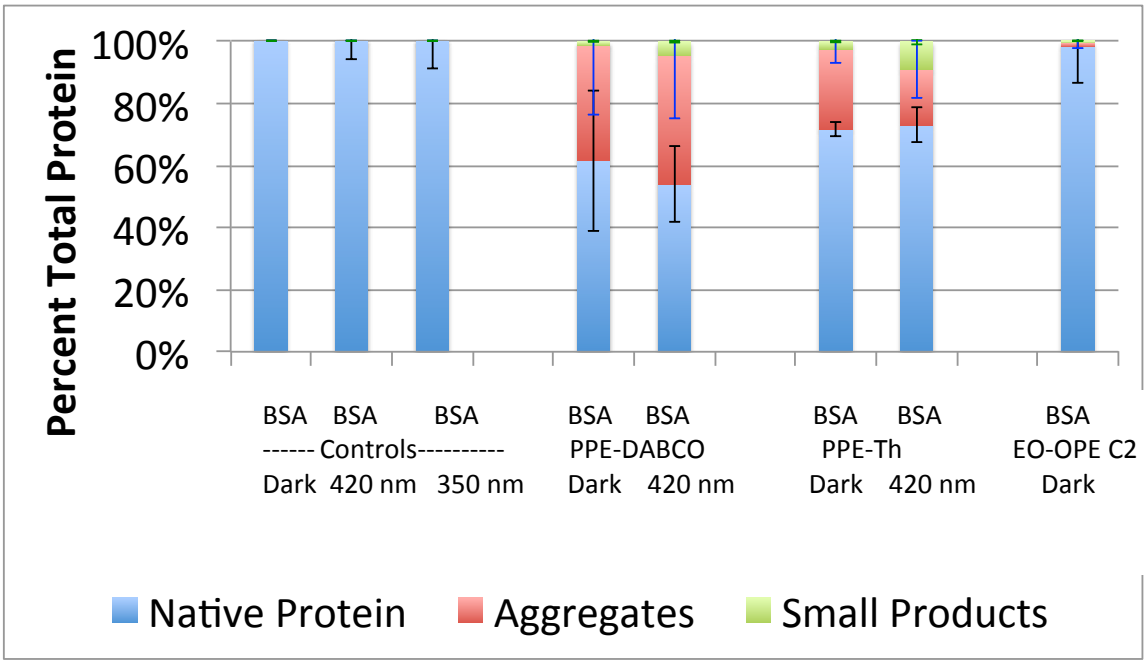

Figure 27: Total BSA percentage loaded on the HPLC accounting for both insoluble and soluble aggregates and small product formation. The effect of irradiation does not change the result.

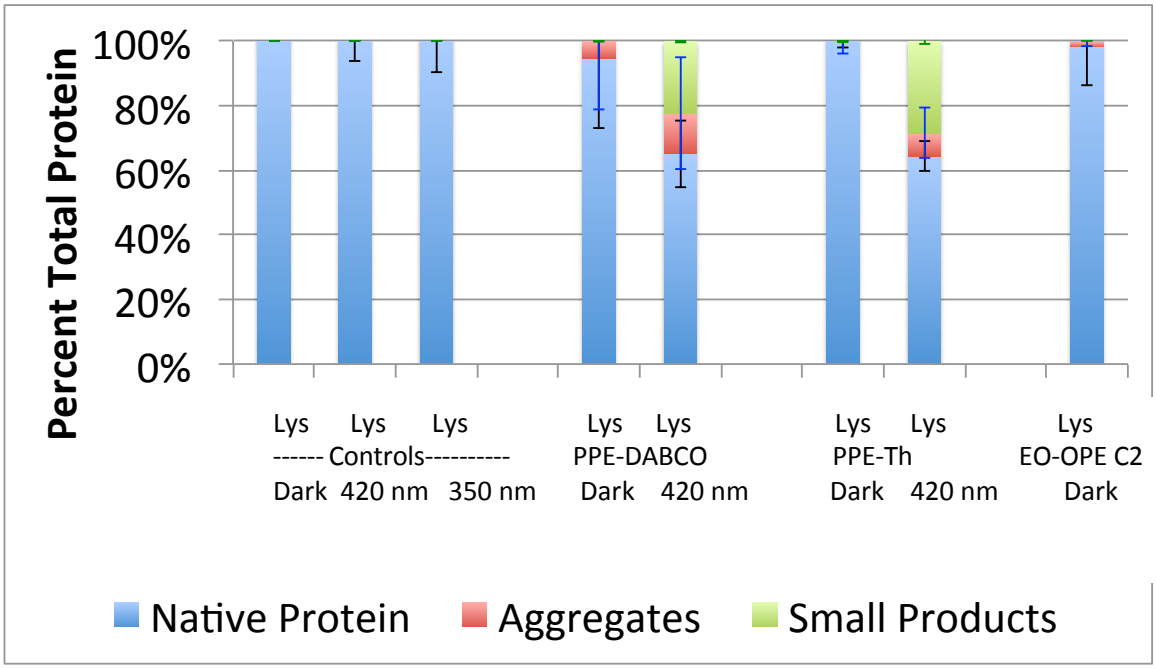

Figure 28: Total lysozyme percentage loaded on the HPLC accounting for both insoluble and soluble aggregates and small product formation. Lysozyme is only affected after irradiation as both polymers have increased aggregate formation and small products.

Both of the tested proteins resulted in supporting data for the SDS-PAGE experiments conducted. Along with the accompanying light scattering result the molecular mass of the soluble aggregates and small products could be determined.

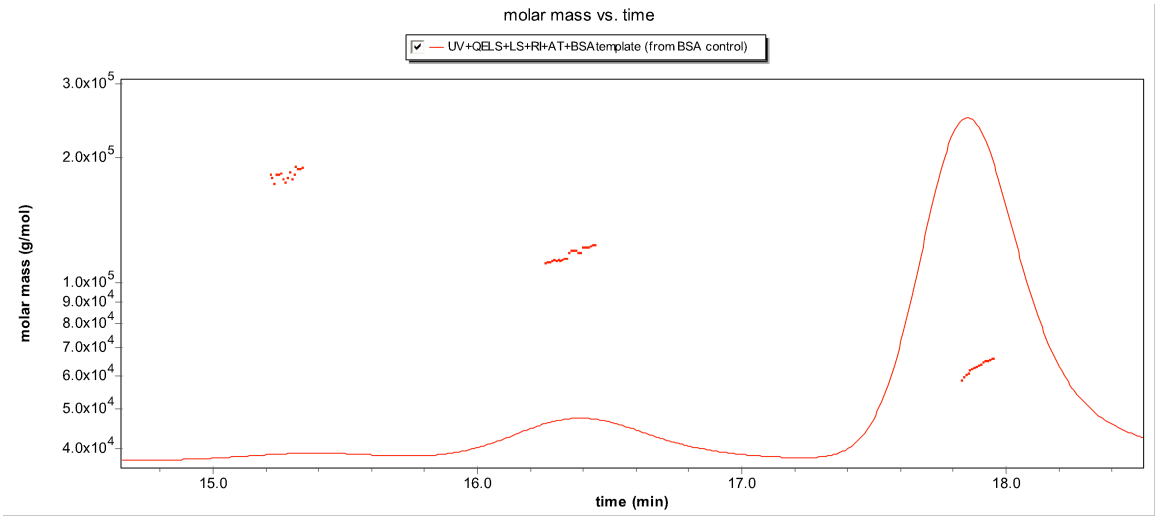

Figure 29: This is a molar mass vs time for the Dawn Heleos-II of BSA control. Displayed is the UV chromatograph collect form HPLC with the clusters showing mass. 100 µg of protein have been loaded to collect data. On this we have starting from the left trimer peak (182 kDa), dimer peak (117.3 kDa), and monomer peak (62.9 kDa) for BSA.
All the values for the control match with literature values. **Figure 30** shows the results for the irradiated PPE-DABCO sample with BSA as that resulted in both soluble aggregates and small products.

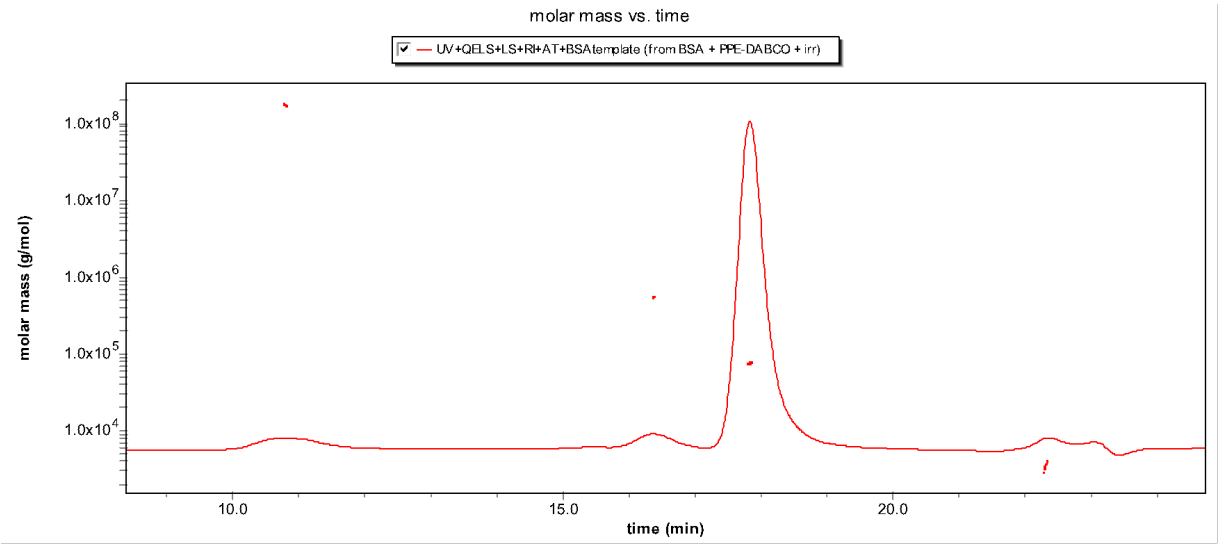

Figure 30: This is a molar mass vs time for the Dawn Heleos-II of BSA with PPE-DABCO after irradiation. Displayed is the absorbance data collect form HPLC with the clusters showing the mass distribution. 100 µg of protein to 10 µg of PPE-DABCO have been loaded to collect data. On this we have starting from the soluble

aggregate (175E3 kDa), trimer/dimer peak (551 kDa), and monomer peak (71.58 kDa) and small product (N/A) for BSA. The two smaller peaks did not return values. These larger values for the trimer, dimer, and monomer peak are most likely a contribution of the compound interacting with the protein. As seen in previous experiment the compound interacts and disrupts the structure of the protein. However, there is a large aggregate being formed that was not removed in the centrifugation step as well as small products that maybe the product from the compound producing reactive oxygen species and resulting in oxygen mediated damage to the protein. **Figures 31 and 32** show the native protein for lysozyme and lysozyme with PPE-Th irradiated as that sample resulted in a 34% of small product formation.

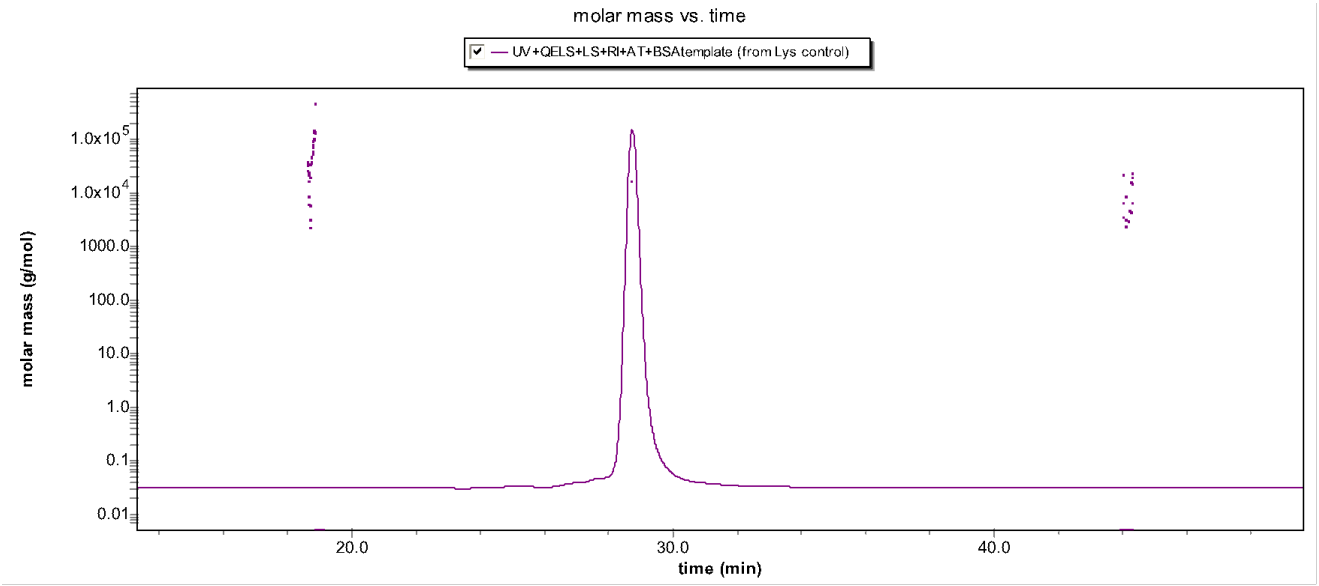

Figure 31: This is a molar mass vs time for the Dawn Heleos-II of Lysozyme control. Displayed is the absorbance data collect form HPLC with the clusters showing the mass distribution. 100 μg of protein have been loaded to collect data. There is a single peak for lysozyme the monomer peak (14.49 kDa).

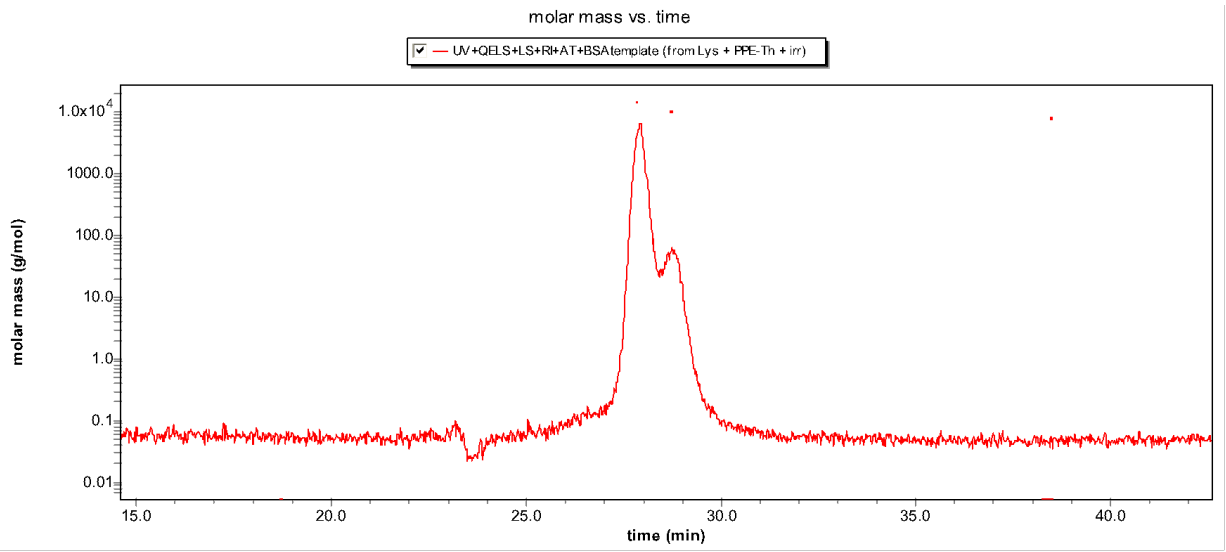

Figure 32: This is a molar mass vs time for the Dawn Heleos-II of Lysozyme with PPE-Th after irradiation. Displayed is the absorbance data collect form HPLC with the clusters showing the mass distribution. 100 μg of protein and 10 μg of PPE-Th have been loaded to collect data There are two peaks for lysozyme the monomer peak on the left (14.23 kDa) and smaller product at (10.16 kDa). This mass difference as before can be contributed to the interaction of PPE-Th and protein.

5. Discussion

While the study began with previous research conducted on model bacteria phages, the mechanism by how the phages were inactivated was unknown. This lead to the research into how proteins are effect by the compound of interest. BSA and lysozyme were chosen due to their function and properties that would make them ideal to investigate. BSA is a globular protein used as a carrier protein in the body contain several α-helical structure making it a very structures protein and contains multiple binding domains that hydrophobic molecule can attach. The fact that BSA is more hydrophobic than lysozyme will allow it to better model membrane proteins. Lysozyme is a small and stable enzyme that functions by providing a defense against gram-positive bacterium by cleaving peptidoglycans. The other important case is that they are oppositely charged. Under the conditions tested BSA has an isoelectric

point of 4.7 has a net negative charge and lysozyme has an isoelectric point of 11.35 a net positive charge.

The chosen studied proteins are important because it is then possible to gather information regarding the interaction with the OPE/CPEs. Through the experimentation process we first look at how these two-model proteins structure is affected beginning with CD experiments. This provided valuable insight into how the compound interacts with the protein. For BSA the results were much more drastic, most likely due to the way BSA is structured, result in loss of α-helical structures result in the reduce intensity. Lysozyme however showed little change when interacting with the compounds tested. Initially this is believed to be due an electrostatic interaction preventing the compound from interacting directly with lysozyme. However, there is interaction with the smaller oligomer compounds after irradiation leading to damage to the secondary structure of lysozyme. This in part with enhanced damage done to BSA after irradiation that the by products of the compounds and generation of reactive oxygen species leading to the disruption of the proteins structure[12,16]. Lysozyme did not undergo changes to the secondary structure with the polymers after irradiation. This could be a result of size and space available for the compound to interact with the proteins. Since BSA is a large carrier protein it has the space and design to bind multiple compounds in the domains for hydrophobic compounds. Making it a good candidate for the hydrophobic backbone of the compound to nestle in and bind changing the proteins secondary structure.

The next set of experiments pertained to the tertiary structure of the protein while also monitoring the compounds conformation due to spectral shifts.

Fluorescence was conducted to accomplish this portion of the project. The fluorescence of the proteins comes from the hidden hydrophobic residues producing and intrinsic fluorescence to monitor. Changes in this would then lead to the conclusion that the protein is undergoing structural change exposing those hydrophobic residues to the solvent environment. While monitoring the compound fluorescence spectral shifts and changes in intensity can be attributed to conformational changes to the compound. Generally speaking a red shift would result in a straightening of the compound leading to a longer chromophore while blue shifts will result in more twist in the compound and short chromophores[20].

BSA fluorescence experiments followed the same results as in CD with all the compounds disrupting the tertiary structure of BSA. The trend follows that BSA is not affected by irradiation alone, but the signal is decreased with the compound and then further decreased after the compound is irradiated. Also for the BSA samples the compounds tested experienced a blue spectral shift. After irradiation the shift is more pronounced as the product has been undergone photo degradation. This means that the compound is in a more twisted conformation resulting in the shorter chromophores. The results for lysozyme followed the same trend as BSA with a decrease in fluorescence intensity in the presence of the compound and that being further enhanced from irradiation. The lysozyme samples also contain blue shifts for the compound but not as pronounced as in the BSA samples. The result from fluorescence leads to the thought that main driving force for the interaction between theses compound and proteins is hydrophobicity. This is because both proteins experienced similar results pertaining to the changes to tertiary structure

unfolding and exposing those hydrophobic residues. The next step was to understand what is happing to the protein once it has interacted with the compounds. This was accomplished by using a first pass method in SDS-PAGE and final pass through SEC-HPLC. The SDS-PAGE is a qualitative method for determining if the protein is form aggregates or small products when exposed to the compounds while SEC-HPLC can be used to quantify these changes.

SDS-PAGE resulted in interesting information regarding these compounds. As before BSA was more susceptible to these changes than lysozyme. BSA was more prone to aggregation than lysozyme and BSA underwent aggregation in both PPE-DABCO treatments and the irradiation treatment of PPE-Th and EO-OPE c2. Lysozyme only saw aggregation in the PPE-DABCO samples. Knowing the results from SDS-PAGE gave a better understanding on how the proteins were being affected. Moving on the SEC-HPLC there is a general idea on what to expect when running the samples as far as aggregation and cleavage products. By knowing the amount of protein loaded and proper integration of the absorbance signal we can quantify how much of the protein is in a native structure, aggregate, or cleavage product. BSA was more susceptible to the polymers than the oligomer as was true for lysozyme. An unexpected result was that BSA was more likely to form large aggregates both soluble and insoluble while lysozyme would form cleavage products. Through most of the experimentation process irradiation was not required to see and affect from the tested compounds while with lysozyme the compounds required that assistance. The fact that lysozyme forms cleavage products as a result of the photo degradation products producing reactive oxygen

species that damage the protein[21]. BSA on the other hand seems to be mediated by the initial binding of the compound to protein initiating an aggregation process leading to the disruption of the secondary and tertiary structure of the protein.

6. Conclusion

While the mechanism is still not clear there is more insight on the interaction is taking place. The more hydrophobic protein resulted in more changes to the structure while the less hydrophobic lysozyme was susceptible to the reactive oxygen species generated by the compound during the irradiation process. This leads to the belief that the compound would generally begin the disruption process through hydrophobic forces. The electrostatics will assist in this process but the predominant force is a hydrophobic interaction. More studies need to be conducted to fully grasp how the interaction takes place. However, through the studies conducted in this project a better understanding of which forces involved is gained.

References

1. Center for Disease Control and Prevention. Threat Report 2013. http://www.cdc.gov/drugresistance/threat-report-2013/ (accessed July 2014)
2. Neidell, M.; Cohen, B.; Fruyua Y.; Hill, J.; Jeon, C.; Glied, S.; Larson, E. Cost of Healthcare- and Community- Associated Infections with Antimicorbial – Resistant Versus Antimicrobial Susceptible Organisms *Clinical Infectious Diseases.* **2012**, 55(6), 807-815.
3. Zhang, X.; Li, Z.; Yuan, X.; Cui, Z.; Bao, H.; Li, X.; Liu, Y.; Yang, X. Cytotoxicity and antibacterial property of titanium alloy coated with silver nanoparticle-containing polyelectrolyte multilayer *Master Sci. Eng. C. Master Biol. Appl.* ***2013****, 33,* 2816-2820
4. Mohan, S.; Oluwfemi, O.; George, S.; Jayachandran,V.; Lewu, F.; Songca, S.; Kalarikkal, N.; Thomas, S. Completely green synthesis of dextrose reduced silver nanoparticles, its antimicrobial and sensing properties *Carbohydrate polymers.* **2014,** 106, 469-474.
5. Mohanty, S.; Jena, P.; Mehta, R.; Pati, R.; Banerjee, B.; Patil, S.; Sonawane, A. Cationic antimicrobial peptides and biogenic silver nanoparticles kill mycobacteria without eliciting DNA damage and cytotoxicity in mouse macrophages. *Antimicrobial agents and chemotherapy*. **2013,** 57(8), 3688-3698.

6. Zhao, F.; Shen, G.; Chen, C.; Xing, R.; Zou, Q.; Ma, G.; Yan, X. Nanoengineering of Stimuli-Responsive Protein-Based Biomimetic Protocells as Versatile Drug Delivery Tools *Chemistry-A European Journal*. **2014**, 20(23), 6880-6887
7. Dengler, E.; Liu, J.; Kerwin, A.; Torres, S.; Olcott, C.; Bowman, B.; Armijo, L.; Gentry, K.; Wilkerson, J.; Wallace, J.; Jiang, X.; Carnes, E.; Brinker, C.; Milligan, E. Mesoporous silica-supported lipid bilayers (protocells) for DNA cargo delivery to the spinal cord *Journal of Controlled Release*. **2013,** 168(2), 209-224.
8. Raemdonck, K.; Braeckmans, K.; Demeester, J.; De Smedt, S Merging the best of both worlds: hybrid lipid-enveloped matrix nanocomposites in drug delivery *Chemical Society Reviews*. **2014***,* 43(1), 444-472.
9. Wang, Ying, et al. "Dark Antimicrobial Mechanisms of Cationic Phenylene Ethynylene Polymers and Oligomers against Escherichia coli." *Polymers* 3.3 (2011): 1199-1214.
10. Wang, Ying, et al. "Understanding the Dark and Light-enhanced Bactericidal Action of Cationic Conjugated Polyelectrolytes and Oligomers." *Langmuir* (2012).
11. Wang, Ying, et al. "Membrane perturbation activity of cationic phenylene ethynylene oligomers and polymers: selectivity against model bacterial and mammalian membranes." *Langmuir* 26.15 (2010): 12509-12514.
12. Chemburu, Sireesha, et al. "Light-induced biocidal action of conjugated polyelectrolytes supported on colloids." *Langmuir* 24.19 (2008): 11053-11062.
13. Corbitt, Thomas S., et al. "Conjugated Polyelectrolyte Capsules: Light-Activated Antimicrobial Micro “Roach Motels”†." *ACS applied materials & interfaces* 1.1 (2008): 48-52.
14. Ding, Liping, et al. "Insight into the Mechanism of Antimicrobial Poly (phenylene ethynylene) Polyelectrolytes: Interactions with Phosphatidylglycerol Lipid Membranes†† Langmuir 25th Year: Molecular and macromolecular self-assemblies." *Langmuir* 25.24 (2009): 13742-13751.
15. Ding, Liping, et al. "Insight into the mechanism of antimicrobial conjugated polyelectrolytes: lipid headgroup charge and membrane fluidity effects. *“Langmuir*

26.8 (2009): 5544-5550
16. Wang, Ying, et al. “Cationic Pheylene Ethynylene Polymers and OligomersExhibit efficient Antiviral Activity” *Applied Materials & Interfaces* 3(2011): 2209-2214
17. Correa, Daniel, et al. “The use of circular dichroism spectroscopy to study protein folding, form and function.”*African Journal of Biochemistry Research* Vol 3.(2009); 164-173
18. Hong, Paula, et al. “A Review Size-Exclusion Chromatography for the analysis of Protein Biotherapeutics and their aggregates.”*Journal of Liquid Chromatography & Related Technologies* 35 (2012): 2923-2950
19. Harding, Stephen; Jumel, Kornelia. “Light Scattering” *Current Protocols in Protein Science* 7.8.1-7.8.14 (1998)
20. Tang, Yanli, et al. “Synthesis, Self Assembly, and Photophysical Properties of Cationic Oligo(p-phenyleneethynylene)s” *Langmuir* 27(2011): 4945-4955
21. Davies, Michael. “Singlet oxygen-mediated damage to proteins and its consequences” *Biochemical and Biophysical Research Communications* 305(2003): 761-770